İSTANBUL TECHNICAL UNIVERSITY ★ INSTITUTE OF SCIENCE AND TECHNOLOGY

ADSORPTION SIMULATIONS OF TRICHLOROETHYLENE AND METHYL TERTIARY BUTYL ETHER IN ZEOLITES

M.Sc. Thesis by

Melissa KARAGÖZLÜOĞLU

Department : Chemical Engineering

Programme : Chemical Engineering

Thesis Supervisor: Assoc. Prof. Dr. M. Göktuğ AHUNBAY

JANUARY 2010

İSTANBUL TECHNICAL UNIVERSITY ★ INSTITUTE OF SCIENCE AND TECHNOLOGY

ADSORPTION SIMULATIONS OF TRICHLOROETHYLENE AND METHYL TERTIARY BUTYL ETHER IN ZEOLITES

M.Sc. Thesis by

Melissa KARAGÖZLÜOĞLU

506071034

Date of submission : 25 December 2009
Date of defence examination : 27 January 2010

Supervisor (Chairman) : Assoc. Prof. Dr. M. Göktuğ AHUNBAY (ITU)
Members of the Examining Committee : Assoc. Prof. Dr. Ahmet Sirkecioğlu (ITU)
Prof. Dr. Mine Yurtsever (ITU)

JANUARY 2010

İSTANBUL TEKNİK ÜNİVERSİTESİ ★ FEN BİLİMLERİ ENSTİTÜSÜ

TRİKLORETİLEN VE METİL TERSİYER BÜTİL ETERİN ZEOLİTLERDE ADSORPSİYON SİMÜLASYONLARI

YÜKSEK LİSANS TEZİ

Melissa KARAGÖZLÜOĞLU

506071034

Tezin Enstitüye Verildiği Tarih : 25 Aralık 2009
Tezin Savunulduğu Tarih : 27 Ocak 2010

Tez Danışmanı : Doç. Dr. M. Göktuğ AHUNBAY (İTÜ)
Diğer Jüri Üyeleri : Doç. Dr. Ahmet Sirkecioğlu (İTÜ)
Prof. Dr. Mine Yurtsever (İTÜ)

OCAK 2010

FOREWORD

I would like to express my deep appreciation and thanks for my advisor Associate Professor Doctor Mehmet Göktuğ Ahunbay for his patience, guidance, reviewing and editing of the manuscript and supervision throughout my graduate dissertation.

I am also grateful to my friends for their motivation and invaluable encouragement during this study.

Last but not least, I offer my grateful thanks to my beloved family; for their unwavering support and love.

I acknowledge the financial support from the Scientific and Technological Research Council of Turkey (TÜBİTAK) through the project with grant number 106M339.

December 2009

Melissa Karagözlüoğlu

Chemical Engineering

TABLE OF CONTENTS

Page

ABBREVIATIONS ..... **vii**
LIST OF TABLES ..... **ix**
LIST OF FIGURES ..... **xi**
LIST OF SYMBOLS ..... **xi**
SUMMARY ..... **xv**
ÖZET ..... **xiv**
1. INTRODUCTION **1**
2.BACKGROUND **7**
3. MOLECULAR SIMULATION **11**
3.1 Statistical Ensembles 12
3.2 Molecular Forcefield 13
3.3 Periodic Boundary Conditions 16
3.4 Ewald Sum 17
3.5 Monte Carlo Method 18
3.5.1 Monte Carlo and ensemble behavior 19
3.5.2 Sampling in Monte Carlo method 20
3.5.3 Metropolis algorithm 22
3.5.4 Monte Carlo moves 23
3.3.5 Averages and error estimations 25
3.6 Molecular Dynamics Method 26
3.6.1 Integrating the equations of motion 27
3.6.2 Verlet algorithm 27
3.6.3 Molecular dynamics and ensemble behavior 28
3.6.4 Diffusion coefficient 30
4. ADSORPTION SIMULATIONS **31**
4.1 Faujasite Structure 32
4.2 ZSM-5 Structure 32
4.3 Simulation Method 33
4.4 Results and Discussions 35
5. DIFFUSION SIMULATIONS **47**
5.1 Simulation Method 47
5.2 Results and Discussions 49
6. CONCLUSIONS **57**
REFERENCES **61**
CURRICULUM VITAE **67**

ABBREVIATIONS

AA	**:** All atoms
AUA	**:** Anisotropic united atoms
CAA	**:** Clean air act
COMPASS	**:** Condensed-phase optimized molecular potential for atomistic simulation studies
CNS	**:** Central nervous system
CVFF	**:** Consistent-valence force field
CVOC	**:** Chlorinated volatile organic compound
DAY	**:** Dealuminated Y
EDF	**:** Equal distribution function
EPA	**:** Environmental Protection Agency
EU	**:** European Union
FDA	**:** Food and drug administration
GAC	**:** Granular activated carbon
GCMC	**:** Grand Canonical Monte Carlo
LJ	**:** Lennard-Jones
MC	**:** Monte Carlo
MD	**:** Molecular dynamics
MOR	**:** Mordenite
NCI	**:** National cancer institute
NOM	**:** Natural organic matter
MSD	**:** Mean square displacement
MTBE	**:** Methyl tertiary butyl ether
NPT	**:** Isothermal-isobaric ensemble
NVE	**:** Microcanonical ensemble
NVT	**:** Canonical ensemble
PBC	**:** Periodic boundary conditions
PCE	**:** Tetrachloroethylene
PCFF	**:** Polymer consistent force field
RDF	**:** Radial distribution function
TBA	**:** Tert-butyl alcohol
TCE	**:** Trichloroethylene
UA	**:** United atoms
USA	**:** United States of America
VOC	**:** Volatile organic compound

LIST OF TABLES

Page

Table 3.1 : Statistical ensembles.....12
Table 4.1 : Properties for zeolites used in adsorption simulations 34
Table 4.2 : LJ parameters and elementary charges of atoms used in the adsorption simulations 34
Table 4.3 : Number of TCE and water molecules adsorbed in ZSM-5 zeolites.....40
Table 5.1 : Numerical values for diffusion coefficients.....49
Table 5.2 : Diffusion coefficient values of water compared to former studies 53

LIST OF FIGURES

Page

Figure 1.1 : Molecular structure of TCE. 1
Figure 2.1 : Molecular structure for MTBE 4
Figure 3.1 : Potential energy plot versus intermolecular distance. The solid curve is LJ, the dashed curve is the Buckingham potential.....15
Figure 3.2 : Intramolecular energy terms for flexible molecules 16
Figure 3.3 : General MC moves. (a) initial configuration (b) translation (c) rotation (d) volume exchange 25
Figure 4.1 : Faujasite structure. 32
Figure 4.2 : A silicalite super cell composed of eight (2x2x2) unit cells along the (a) x-direction (b) y-direction (c) z-direction 33
Figure 4.3 : Adsorption isotherms of MTBE with respect to temperature 36
Figure 4.4 : Adsorption isotherms of MTBE with respect to zeolite structure 37
Figure 4.5 : Adsorption isotherms of TCE in faujasites 38
Figure 4.6 : Adsorption isotherms of TCE in DAY.....38
Figure 4.7 : Concentration profiles of TCE in faujasites 38
Figure 4.8 : Adsorption isotherms of TCE and water in ZSM-5.....39
Figure 4.9 : Concentration profiles of TCE adsorbed in ZSM-5 zeolites, with respect to adsorbed TCE, aligned by the projection of ZSM-5 zeolite on yz-plane 41
Figure 4.10 : Concentration profiles of molecules and cations in ZSM-5 zeolites with respect to zeolite type 42
Figure 4.11 : Snapshot pictures from the simulation box of ZSM-5 - TCE - water system. (a) silicalite (b) NaZSM-5 (191) (c) NaZSM-5 (95) 43
Figure 4.12 : Change in RDFs of hydrogen atoms in TCE molecules with alumina content 43
Figure 4.13 : Change in RDFs of oxygen atoms in water molecules with alumina content 44
Figure 4.14 : A NaZSM-5(95) composed of eight (2x2x2) unit cells along the (a) x-direction (b) y-direction (c) z-direction, Al atoms located along only the sinusoidal channels.....44
Figure 4.15 : A NaZSM-5(95) composed of eight (2x2x2) unit cells along the (a) x-direction (b) y-direction (c) z-direction, Al atoms located along both elliptical and sinusoidal channels 45
Figure 4.16 : Adsorption isotherms of aqueous TCE in NaZSM-5 (95) for different Al locations at 298K, compared to the previous isotherms.....45
Figure 4.17 : Adsorption isotherms of water in NaZSM-5 (95) for different Al locations at 298K, compared to the previous isotherms 46
Figure 5.1 : Two (1x1x2) unit cells of silicalite with (a) pure TCE (b) water and TCE molecules adsorbed.....48
Figure 5.2 : Two (1x1x2) unit cells of silicalite with water molecules adsorbed ...48
Figure 5.3 : Diffusion coefficients of TCE 50

Figure 5.4 : Concentration profiles of TCE diffused into ZSM-5 zeolites at 298K and 348K, with respect to adsorbed TCE 51
Figure 5.5 : Concentration profiles of TCE diffused into ZSM-5 zeolites at 298K and 348K, with respect to zeolite type..... 51
Figure 5.6 : MSD-time graphics of TCE for different electrostatic charges of silicon atoms..... 52
Figure 5.7 : Diffusion coefficient distribution of TCE depending on the partial charge of Si atoms in silicalite framework..... 53
Figure 5.8 : Concentration profiles of water molecules diffused into silicalite..... 54
Figure 5.9 : Comparison of RDFs of oxygen atoms in water molecules diffused into silicalite 54
Figure 5.10 : RDFs of oxygen atoms in water molecules diffused into silicalite framework with different partial charges of Silicon atoms 55

LIST OF SYMBOLS

A	: A property
a	: Acceleration
a	: A positive constant
c	: A positive constant
C_p	: Specific heat at constant pressure
C_v	: Specific heat at constant volume
D	: Diffusion coefficient
E	: Potential energy
f	: A function
F	: Force
H	: Enthalpy
k	: Thermal conductivity
k_B	: Boltzmann constant
K_A	: Actual kinetic energy
k_{bend}	: Bending constant
K_D	: Desired kinetic energy
L	: Box length
m	: Interaction number
m	: A constant number
m	: Mass
N	: Number of particles or molecules
P	: Pressure
p	: Probability
P_{acc}	: Acceptance probability
q	: A random number
q	: Partial charge
r	: Distance
r	: Position
R	: Random numbers
t	: Time
T	: Temperature
u	: Increase in potential energy with addition of a particle
U	: Potential energy
U^{bend}	: Bending energy
$U_{d\text{-}r}$	: Dispersion-repulsion energy
U_{el}	: Coulombic energy
U_{ext}	: Intermolecular potential energy
U_{int}	: Intramolecular potential energy
u_{LJ}	: Lennard-Jones force center interaction energy with system
U_{pol}	: Polarization energy
U^{tors}	: Torsion energy
v	: Velocity
V	: Volume

V_{Buck} : Buckingham potential
X : A property
Z : Participation function
β : Probability density (Boltzmann factor)
ΔV : Volume change
ε : LJ well depth
ε_0 : Electrostatic constant
θ : Bending angle
θ_0 : Equilibrium bending angle
μ : Chemical potential
μ : Arithmetic average
μ : Viscosity
ρ : Phase density
ρ : Probability density
ρ : Characteristic distance
σ : LJ size
σ^2 : Variance
ϕ : Dihedral angle

ADSORPTION SIMULATIONS OF TRICHLOROETHYLENE AND METHYL TERT BUTYL ETHER IN ZEOLITES

SUMMARY

Methyl tertiary butyl ether (MTBE) and trichloroethylene (TCE) are volatile organic compounds, which are used in various branches of industry. After their usage for several years, unexpected health problems have occurred in humans. TCE was found to be carcinogen and toxic, also affecting the central nervous system. TCE was detected in groundwater resources. Apart from TCE, MTBE usage in high concentrations resulted in many health complaints. It was reported to cause a variety of cancer types. It was detected in many water resources. The presence of MTBE and TCE in water resources has interested the scientists for the removal studies. Adsorption of these molecules onto surfaces is one of the treatment processes. The advantage of the adsorption processes is that no byproducts are produced. High-silica zeolites, such as ZSM-5 and DAY (dealuminated Y) have successfully removed TCE and MTBE from water in previous experimental works.

In chemical engineering, molecular simulation methods are widely used to determine thermophysical properties. Compared to experiments, simulations provide saving of time, and are also advantageous economically. Especially Grand Canonical Monte Carlo method is used to simulate adsorption of guest molecules in various nanoporous materials. Simulations of diffusion systems are performed using molecular dynamics method.

In this work, adsorption and diffusion simulations are performed. Except for silicalite structure, sodium atoms are used as the extraframework cations. Adsorption simulations result in isotherms, which give information about the adsorption properties of the molecules studied. On the other hand, diffusion simulations are performed in order to calculate diffusion coefficients of TCE and water. Adsorption and diffusion properties of pure TCE and its aqueous mixture in ZSM-5 are investigated compared to silicalite; the all silica version of ZSM-5. Pure TCE saturation in ZSM-5 is around 9 molecules per unit cell. For aqueous TCE adsorption simulations in ZSM-5, TCE loading increases while water loading decreases. The presence of water results in a decrease in TCE diffusion coefficient. However, temperature does not have a significant effect. In addition, pure water diffusion behavior in silicalite is investigated with respect to changing partial charges in the zeolite structure. Pure TCE and MTBE adsorptions in faujasites (FAU) are also analyzed separately. As a result of these simulations, it is found that MTBE adsorption in faujasites increases with decreasing Si/Al ratio. However, a saturation capacity of 30 MTBE molecules per unit cell is observed for all MTBE adsorption simulations. TCE adsorption in DAY is found to be in good agreement with previous experimental studies. In water diffusion simulations, diffusion coefficient is observed to be decreasing with increasing partial charge of silicon atoms.

TRİKLORETİLEN VE METİL TERSİYER BÜTİL ETERİN ZEOLİTLERDE ADSORPSİYON SİMÜLASYONLARI

ÖZET

Metil tersiyer bütil eter (MTBE) ve trikloroetilen (TCE), sanayinin birçok alanında kullanılan uçucu organik bileşiklerdir. Yıllarca kullanılmalarının ardından, insanlarda beklenmedik sağlık problemleri meydana gelmiştir. TCE'nin kanserojen ve toksik olduğu, merkezi sinir sistemini etkilediği belirlenmiştir. TCE yer altı su kaynaklarında bulunmuştur. TCE'nin yanı sıra MTBE'nin yüksek konsantrasyonlarda kullanımı birçok sağlık şikayetine yol açmıştır. MTBE'nin çeşitli kanser türlerine sebep olduğu gözlemlenmiştir. Birçok su kaynağında bulunduğu tespit edilmiştir. MTBE ve TCE'nin su kaynaklarındaki mevcudiyeti, bilim insanlarının giderme çalışmalarına ilgisini çekmiştir. Bu moleküllerin yüzeye adsorpsiyonları işleme süreçlerinden biridir. Adsorpsiyon süreçlerinin avantajı, herhangi bir yan ürünün üretilmiyor olmasıdır. Önceki deneysel çalışmalarda ZSM-5 ve DAY (dealümine edilmiş Y) gibi yüksek silikalı zeolitler TCE ve MTBE'yi başarıyla sudan uzaklaştırmışlardır.

Kimya mühendisliğinde moleküler simülasyon metotları termofiziksel özelliklerin belirlenmesinde sıkça kullanılmaktadır. Deneylerle kıyaslandığında, simülasyonlar zamandan tasarruf sağlarlar ve ekonomik açıdan avantajlıdırlar. Konuk moleküllerin çeşitli nano gözenekli malzemelere adsorpsiyonunun benzetiminde özellikle Büyük Kanonik Monte Karlo yöntemi kullanılmaktadır. Difüzyon sistemlerinin benzetimleri moleküler dinamik yönteminin kullanılması ile yürütülmektedir.

Bu çalışmada, adsorpsiyon ve difüzyon benzetimleri yürütülmüştür. Silikalit yapısı haricinde, ekstra iskelet yapısı katyonları olarak sodyum atomları kullanılmıştır. Adsorpsiyon benzetimleri, çalışılan moleküllerin adsorpsiyon özellikleri hakkında bilgi veren izotermlerle sonuçlanmaktadırlar. Öte yandan, TCE ve suyun difüzyon katsayılarını hesaplamak için difüzyon benzetimleri yürütülmektedir. Saf TCE ve sulu çözeltisinin ZSM-5 zeolitine adsorpsiyon ve difüzyon özellikleri, ZSM-5'in tüm silika modeli olan silikalite kıyasla incelenmiştir. Saf TCE'nin ZSM-5 zeolitindeki doygunluk kapasitesi birim hücrede yaklaşık 9 moleküldür. TCE'nin ZSM-5 zeolitine sulu adsorpsiyon benzetimlerinde su yüklemesi azalırken TCE yüklemesi artar. Suyun varlığı TCE'nin difüzyon katsayısında düşüşe sebep olur. Ancak, sıcaklık dikkate değer bir etkiye sahip değildir. Bunun yanısıra, saf suyun silikalitte difüzyon özellikleri zeolit yapısındaki kısmi yüklerin değişimine bağlı olarak incelenmiştir. Fojasite (FAU) saf TCE ve MTBE adsorpsiyonları ayrı ayrı analiz edilmiştir. Bu benzetimlerin sonucunda, fojasite MTBE adsorpsiyonunun azalan Si/Al oranı ile arttığı görülmüştür. Ancak, tüm MTBE adsorpsiyon benzetimleri için doygunluk kapasitesi birim hücrede 30 MTBE molekülü olarak gözlemlenmiştir. DAY'da TCE adsorpsiyonunun önceki deneysel çalışmalar ile uyumlu olduğu görülmüştür. Su difüzyon benzetimlerinde difüzyon katsayısının artan silikon yükü ile azaldığı gözlemlenmiştir.

1. INTRODUCTION

In industry, volatile organic compounds (VOCs) are produced commercially and used in many fields. Trichloroethylene (TCE) which is a chlorinated hydrocarbon, is one of the chlorinated volatile organic compounds (CVOCs) and is widely used as an industrial solvent mostly for vapor degreasing and cold cleaning of fabricated metal parts, in case, is primarily released to environment from metal degreasing plants. It can exist in the wastewater from operations such as textile cleaning, paint and ink formulation, rubber processing, metal finishing and electrical/electronic equipment. It is not a persistent chemical in the atmosphere; with a half-life in air about 7 days. It is colorless and has a sweet odor like ether or chloroform. The odor threshold is 28 ppm. Its molecular weight is 131.39 g/mole, its structural formula is shown in Figure 1.1. Its solubility in water is approximately 1.280 g/L at room temperature. It is soluble majorly in diethyl ether, ethanol, acetone, and chloroform [1-5]. It does not occur in the environment naturally. However, as an exception, TCE is found to be naturally produced in temperate, subtropical and tropical algae and in one red microalgae. The manufacturing, use, and disposal of chemicals lead to TCE presence in groundwater sources. TCE does not evaporate from subsurface soils easily and can reach the groundwater [2].

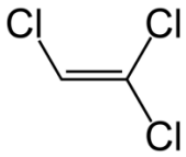

Figure 1.1 : Molecular structure of TCE

The main preference reason of TCE in industrial use is its low flammability, noncorosivity and reactivity, easily recyclability. It can dissolve a large variety of organic substances efficiently [6,7].

TCE can be obtained from many processes. It is the co-product of a multi-step process, which starts with the chlorination of acetylene and continues by lime

dehydrochlorination and chlorination. This method was not used after 1970s owing to the high cost of acetylene [7]. TCE can also be produced from the chlorination or oxychlorination of ethylene or 1,2-dichloroethane. The first TCE was prepared by E. Fischer in 1864 by the reductive dehalogenation of hexachloroethane [6].

The commercial use of TCE started in early 1900s. The first reported TCE plant started working in 1908 in former Yugoslavia. In late 1920s, industrial use of TCE started by the developments in metal degreasing. In 1927, it started to be used in food industry for the extraction of natural fats and palm, coconut and soybean oils [6].

In 1930s, TCE was used in dry-cleaning as an alternate for flammable petroleum distillates. Its toxicity was discovered in mid-1930s. In 1940s, TCE popularity in metal degreasing increased rapidly, but it posed danger in dry-cleaning, because it was penetrating into certain types of cellulose acetate dyes. In the United States of America (USA), 1970 was the year for maximum TCE usage. However, parallel to the regulatory and economic effects, a decrease was observed. The Clean Air Act (CAA) brought some limitations for TCE due to causing the formation of ozone and smog. In 1975, National Cancer Institute (NCI) brought to the agenda that TCE was effective in cancerous tumor growths in mice livers. Consequently, in 1976, Environmental Protection Agency (EPA) added TCE to the Hazardous Substance List. Besides, General Foods Corporation and Food and Drug Administration (FDA) notified that they ceased TCE usage. Plants using acetylene for TCE production shut down due to high acetylene cost. As expected, TCE price doubled between 1975-85. However, USA decreased TCE production owing to limitations on emissions and usage of other solvents instead [1].

TCE and methyl chloroform, which is another chlorinated hydrocarbon, are produced about 80.000-100.000 tons a year in Japan. They are observed in USA and Japan groundwater and environmental contamination caused by them has been a serious problem. The permissible concentration for TCE in working area is set at 50 ppm by Japan Association of Industrial Health. In the USA, it is set at 10 ppm by American Conference of Governmental Industrial Hygienists [8].

TCE is known to be a carcinogenic substance and if found in amounts greater than the health standard set by the USA EPA, it may cause health problems [3,4]. Acute (short-term) and chronic (long-term) inhalation of TCE can show symptoms such as dizziness, headaches, confusion, euphoria, facial numbness, and weakness while

affecting the human central nervous system (CNS). In addition, immunological, endocrine, and developmental effects have been detected in humans. In a recent study, it is reported that TCE exposure is associated with several types of cancers in humans, especially kidney, liver, cervix, and lymphatic system. The detection of TCE in human body can be achieved by measuring it in the breath, and breakdown products of it can be measured in urine or blood [5].

The emitted TCE intends to part in the atmosphere. It is accepted that 60%-90% of worldwide annual TCE production is released to the environment. The reduction of TCE is related to atmospheric photooxidation. High vapor pressure and low solubility in water are the pivotal points for TCE treatment. Due to its high volatility, TCE releases from surface waters into the air. The evaporation rate is related to wind speed, the flow characteristic of the water, and the temperature of the medium. Photodegradation and hydrolysis processes are not effective in TCE removal, because they are slow and insufficient [1].

Adsorption is accepted to be the most effective process for CVOC control. Other remediation methods for TCE are air stripping, soil venting, surface bioreactors, and in situ bioremediation. Treatments for contaminated water are applied by air stripping, carbon adsorption, and surface bioreactors. Soil venting is used for contamination in the vadose zone. In situ bioremediation can be used in the vadose zone and in the water table [9]. Among all these, the primary solution for CVOCs removal is known to be the activated carbon adsorption. Though, it has some disadvantages such as pore blocking, hygroscopicity, and combustion at high temperatures [3]. As an alternative to these usual processes, zeolites have started to be used for CVOCs separation. It has aroused interest to use hydrophobic zeolites such as ZSM-5, silicalite, and dealuminated Y (DAY) for the removal of CVOCs [10,11].

Another VOC considered in this study is methyl tertiary butyl ether (MTBE). Since 1979, it has been used as a fuel additive in order to increase the oxygenate amount and to replace lead in the gasoline. Oxygenate plays role in reducing harmful tailpipe emissions. In 1990s, the motor gasoline consisted of 15% MTBE in volume. MTBE has suitable blending characteristics for this use and is also advantageous economically [12,13]. It is an aliphatic ether, being in liquid phase at room temperature. It is formed by the reaction of isobutylene and methanol [14]. It has a

low molecular weight (88.15 g/mole), its molecular structure can be seen in Figure 1.2. It is colorless and has a characteristic odor. It can combust when exposed to heat or fire, is highly flammable. Fire can result in toxic gases. MTBE is highly volatile and vapor MTBE can lead to explosive mixtures when combined with air. As another disadvantage, it is unstable in acid solutions. Besides its miscibility in gasoline, MTBE is soluble in water, with approximately 50 g/L solubility at room temperature, alcohol, and other ether types [15].

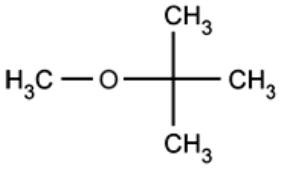

Figure 1.2 : Molecular structure for MTBE

In the areas where it is used as a fuel additive, MTBE occupies 5-10% of the VOCs emitted to air from gasoline burning vehicles. It is not known to bioaccumulate in fish or food chains, so foodstuff is not under the threat of MTBE [12,13].

The commercial production of MTBE started in 1973 in Europe, and in 1979 in USA. In 1998, the production capacity in the world was 23.5 million tonnes with an actual production of 18 million tonnes. This number was doubled in 1992. This increase of MTBE demand was an outcome of USA CAA. TCE has been present in gasoline in amounts up to 15% by volume since then [14].

As mentioned before, MTBE was being used for decreasing air pollution. However, MTBE released to the environment has contaminated the drinking water resources. In 1992, followed by the usage of high concentrated gasoline, some acute health symptoms were reported in USA. Contamination reports were drown up for the water supplies from underground storage tanks in 1996 in USA. Meanwhile, it was proved that MTBE was a carcinogen compound, and also changed the taste of the drinking water. In liquid or gaseous state, it can easily be absorbed into the blood stream [16,17]. MTBE absorption into the cardiovascular system is possible via inhalation or ingestion. After absorption, MTBE demethylates and forms tertiary-butyl alcohol (TBA) and formaldehyde. The chemical reductions of these molecules can lead to carbon dioxide which results in toxicity. Consequently, EPA has set a concentration limit for MTBE: 20 μg/L for odor and 40 μg/L for taste concerns. In Japan, the commercial fuel content by MTBE was decreased to 7% [12,13,18,19].

MTBE has a high mobility owing to its high aqueous solubility, low Henry constant, small molecular size, and relative resistance to biodegradation. Its low volatility makes it difficult to be removed from water by air stripping and active carbon. Besides; biodegradation and chemical oxidation processes produce byproducts of MTBE like metabolites, tert-butyl alcohol (TBA), and bromate, which are hazardous and necessitate removal that means expense. In air stripping, MTBE moves from aqueous phase to aero, by the adsorption columns. This seems to be an economic method, but the waste gas constitutes an environmental problem, also, the separation process is not sufficiently effective at low temperatures. Although activated carbon is used for the purification in a wide range, it is not efficient enough for MTBE removal [18,20,21].

Aforementioned processes are insufficient for MTBE removal. An alternative is the adsorption technique on special structures. By adsorption, MTBE is caught on surfaces. Likely, the best results are obtained by using high-silica zeolites, which are microporous materials. Some recent studies over this process are described in the following chapter.

Some chemical engineering studies are carried out using molecular simulation techniques. They give information about the bulk system, by working on small systems in nano scale. They constitute a connection between experimental data and molecular structure [22]. The adsorption of hydrocarbons in zeolites is applied in petrochemistry. Grand Canonical Monte Carlo (GCMC) simulations can describe the adsorption of hydrocarbons in zeolites [6,7].

The objective of this study is to investigate the adsorption properties of two VOCs TCE and MTBE in hydrophobic zeolite ZSM-5 and faujasite. The effect of changing Si/Al ratio on adsorption is especially examined. Besides, aqueous adsorption and diffusion simulations are carried out, resulting in the determination of water effect. In addition, the effect of changing charges of zeolite atoms on the water adsorption is investigated. Monte Carlo (MC) and molecular dynamics (MD) simulations are introduced for these purposes.

Zeolites are crystalline aluminosilicate materials that have uniform nanopores. Their importance comes from the compatibility to separate different types of molecules. They act as a selective catalyst and adsorbent by usually being used in adsorption

and diffusion processes [23,24]. They have TO_4 (T=Si or Al) tetrahedra, and these are connected to each other over the oxygen atoms. In this connection way and by T=Si, a completely siliceous structure is obtained resulting in silica (SiO_2) which is an uncharged solid. As aluminum atoms are replaced with silicon atoms, cations are added in order to keep the framework neutral. Generally, the zeolite composition can be shown as in Equation 1.1,

$$M_{n/m}^{m+} \cdot [Si_{192-n}Al_nO_{384}] \cdot nH_2O \quad \textbf{(1.1)}$$

where M represents the extraframework cation with charge *m*, and *n* is the number of Al atoms in the framework. The Si/Al ratio can change from 1 to infinity, which results in completely siliceous structure. Hydrothermal stability and so hydrophobicity increases by increasing Si/Al ratio [25].

2. BACKGROUND

Zeolites are microporous, aluminosilicate materials with uniform pores, commonly used as commercial adsorbents. They are compatible to separate different types of molecules. They are usually used in adsorption and diffusion processes for purification of an environment from undesirable molecules. They have selectivity for certain molecules. The hydrophobic molecular sieves are particularly important, because they can be used for the separation of organics from water. Their major advantageous properties are stability, incombustibility, hydrophobicity and low temperature of regeneration [26]. In this section, some recent studies about the adsorption of organic molecules relative to the cases covered in this study are summarized.

For TCE adsorption, many experiments have been performed in comparison with different adsorbents under different conditions. In an early study, the adsorption isotherms of TCE and tetrachloroethylene (PCE) in ZSM-5 (Si/Al=339) were measured by Bouvier and Weber [27]. They found that the shape of the isotherm depended on the polarity of the molecule. For TCE, channel type was not effective in filling the zeolite micropores, but for PCE, a stepped isotherm was obtained. They concluded that zeolite symmetry played a role in this difference [27].

In another study, adsorption of CVOCs was investigated by Clausse *et al.* [28]. They showed that DAY acted as a hydrophobic solvent in the adsorption process. They claimed that the adsorption selectivities and separation processes of a mixture of certain CVOCs could be predicted by knowing the physical properties of single chemicals [28]. In consistence, Garrot *et al.* [26] argued that DAY and siliceous ZSM-5 (DAZ) selectively adsorbed CVOCs. However, they behaved differently. For CVOC mixtures, DAY was selective for the least water-soluble VOC. In an environment of adsorbent mixture, the least volatile would be captured in the zeolite, and the most volatile would escape [26].

In 2000, Giaya and Thompson [29] studied the molecular sieves for the adsorption of some CVOCs from water. They concluded that hydrophobic zeolites were better than

activated carbon in adsorbing. This property was more important in low concentrations in vapor or liquid water. Also, they proved that silicalite was more successful at low CVOC concentrations, and DAY was more efficient at high CVOC concentrations [29].

The pure vapor isotherms of TCE with chloroform in silicalite and DAY were also measured by Giaya and Thompson [30]. They stated that both structures had similar loading capacities towards TCE. At lower pressures, silicalite adsorbed more TCE than DAY, owing to its smaller pore diameter. At higher pressures, DAY outperformed silicalite because DAY has larger pore size. For both zeolites adsorbed amount decreased with increasing temperature [30].

In a gas chromatography experiment, Chihara *et al.* [31] used three different zeolites for the adsorption of various CVOCs and found out that the adsorbed amount decreased with increasing SiO_2/Al_2O_3 [31].

In 2007, Ahunbay [11] carried out molecular simulations for the determination of adsorption isotherms and diffusion coefficients of TCE and PCE in ZSM-5 type zeolites. He obtained data consistent with general experimental data. However, simulation accuracy decreased with increasing temperature. He concluded that this was because of the insufficiency of the consistent-valence force field (CVFF) which he used for modeling the system [11].

As mentioned before, MTBE is the other VOC considered in this study. To the date, there have been many publications on the adsorption of MTBE from water in different zeolites, as alternatives to activated carbon. Noack *et al.* [32] studied the methanol-MTBE mixture separation by MFI type zeolites. They justified that MTBE molecules could not pass through the MFI pores effectively, as MTBE had a molecular diameter of 0.63 nm. They also showed that ZSM-5 accepted more MTBE molecules than silicalite did [32].

In another study, Anderson [17] investigated the MTBE adsorption from water in high-silica mordenite (MOR), ZSM-5, and zeolite Y in comparison to Barneby-Cheney and Fischer activated carbons. As a result, mordenite and silicalite performed high adsorption capacity than activated carbons, but mordenite was better than ZSM-5. They also noted that ZSM-5 was the most efficient at TCE removal from TCE-MTBE-chloroform solutions. Mordenite and activated carbon almost adsorbed the

same. The removal amount of TCE and MTBE by activated carbon was found to be increasing with decreasing water solubility [17]. Li *et al.* [33] carried out experiments with three types of zeolite beta: H^+-beta, dealuminated beta, and all-silica beta. They compared their results with Anderson's, and found out that all-silica zeolite beta was better in MTBE adsorption [33].

Erdem-Şenatalar and her coworkers [34] did a comprehensive study on zeolites. They used silicalite, mordenite, zeolite beta, and dealuminated Y (DAY) with SiO_2/Al_2O_3 ratio differing in 80-1000 interval comparing the results with MTBE adsorption from water in Centaur® Activated Carbon obtained from Calgon Corporation. Followed by mordenite, silicalite was the most efficient at low concentrations. On the other hand, DAY showed the best performance at high concentrations. However, it was the worst at low concentrations, because under that condition water molecules were adsorbed in DAY pores. The detection about silicalite was not in agreement with previous works, which concluded that MTBE molecules could not pass through silicalite. They proved this by claiming that a deformation of the molecules, crystal defects, or vibration in the crystal lattice could provide MTBE entrance to the pores. However, the molecule dimension in z-axis was larger than the pore size. As a conclusion of the research, they proved that at low concentrations, SiO_2/Al_2O_3 ratio and small pores were effective on adsorption, on the contrary, large pores and high hydrophobicity were the dominant factors on loading amounts [34].

Knappe *et al.* [35] used the same zeolites that Erdem-Şenatalar *et al.* [34] studied, but they used different types and loadings of cations; H^+, Na^+, NH_4^+ and compared their results with the experiments of MTBE adsorption in different types of activated carbons. Both researchers agreed that especially silicalite performed better than activated carbon adsorbents [35].

In a second study by Rossner and Knappe [36]; silicalite, coconut-shell-based granular activated carbon (GAC), and spherical carbonaceous resin were used for MTBE removal from water. Besides ultrapure water, river water was used for the investigation of natural organic matter (NOM) effect on MTBE adsorption. Silicalite and carbonaceous resin performed better MTBE uptake than GAC [36].

The existence of another molecule in the medium that is aimed to be purified is also effective on adsorption. Gironi *et al.* [37] performed activated carbon experiments

with three mixtures: MTBE-air, 1-methylbutane-air, and MTBE-1-methylbutane-air. They especially used air, because water contamination is partially caused by MTBE present in air. This MTBE emission comes from motor exhaust gases and gasoline stations. The researchers observed that activated carbon showed 55% capacity for MTBE and 45% for 1-methylbutane by weight. As another important result, they proved that 1-methylbutane decreased the MTBE adsorption [37].

As for theoretical studies on MTBE adsorption, Yazaydin and Thompson [38] analyzed the effect of Na^+ cation on loading amounts into the zeolites silicalite, mordenite, and zeolite beta. At low pressures, silicalite and zeolite beta were more effective than mordenite. Zeolite beta adsorbed the most at high pressures; three times larger than silicalite and mordenite which performed almost the same. The high capacity of zeolite beta comes from its large pores. At low pressures, the presence of Na^+ cations improved the loadings except for mordenite. The closely selected aluminum atoms caused the Na^+ cations to close the pore entrances, whereat MTBE could not fill the pores. Also at low pressures, higher loading values were observed in zeolite beta as well as in mordenite, provided that aluminum atoms were far. However, for high pressures the locations of the aluminum atoms did not make much effect [38].

A recently published study on both experimental and theoretical MTBE adsorption was carried out by Ahunbay *et al.* [40]. They exhibited pure MTBE adsorption in silicalite at different temperatures. At 298K, they compared different forcefields and agreed that polymer consistent force field (PCFF) [39] used in simulation was the best for isotherm prediction. Experimental and theoretical results, which agreed with Yazaydin and Thompson's work [38] showed that silicalite could accept a maximum loading of 4 molecules per unit cell. They continued adsorption simulations at high temperatures (425-600K). These also conformed to the experiments, especially at low temperatures and high pressures. However, they did not show consistence at high temperatures and low pressures which means at lower loadings. They also investigated the effects of silicalite symmetry transition, but did not observe any appreciable change [40].

3. MOLECULAR SIMULATION

Thermophysical properties of a system can be predicted by molecular simulation both qualitatively and quantitatively. It is appropriate to describe molecular simulation as computational statistical mechanics. By using molecular simulation, reasonable results can be obtained because in this technique, molecular coordinates of the system develop by the accurate calculation of intermolecular energies or forces. In molecular simulation, a theoretical model of molecular behavior is calculated and the macroscopic property of the system is determined. Provided that there is an incompatibility between the accurate experimental measurements and the molecular simulation data, it is likely to claim that the model representing the molecular behavior is not well defined [26,41].

In the history of technology, as computers have developed, molecular simulation has innovated. In 1953, Metropolis et al. performed the first molecular simulation of a liquid by presenting the Monte Carlo (MC) method. To give a brief information about MC simulation, as it is explained in the following sections, different trial configurations are generated randomly. First, the intermolecular interactions in the trial configuration are calculated, then probabilities are used and accordingly the change is accepted or rejected. In 1957-59, molecular dynamics (MD) method was presented by Alder and Wainwright [41]. MD method is time dependent and can be used to determine equilibrium and dynamic properties like transport coefficients: viscosity, thermal conductivity and diffusion coefficient. In MD, Newton's equations of motion for the particles in the system are integrated with time. The intermolecular forces of the molecules result in changes in molecular coordinates and momenta. On the other hand, MC method can be used for phase equilibria and sorption. MC is the most efficient technique for determining fluid phase equilibria properties. Different from MC, MD is not stochastic but deterministic. Besides, MD is based on intermolecular forces. However, MC is based on the changes in intermolecular energy. In both methods, it is essential to define the potential energy that involves both intermolecular and intramolecular interactions. Both MC and MD methods are based on statistical thermodynamics. Molecular simulation makes predictions about

thermophysical properties in a single theoretical framework; that is called statistical thermodynamics [26,41].

3.1. Statistical Ensembles

There are different statistical ensembles (Table 3.1) which can be used according to the application needed. Statistical mechanics underlie the methods used in molecular sampling. In statistical mechanics, average value of all possible quantum states indicates the macroscopic property of the system. In order to calculate the property of a real system, it is necessary to define an ensemble, which is an imaginary collection of many systems in different quantum states with common macroscopic attributes. For example, each system in the ensemble and the real system it represents must have the same temperature, pressure and number of molecules [26,41].

Table 3.1 : Statistical ensembles [26]

Statistical ensemble	Imposed variables	Applications
Microcanonical ensemble	N, V, E	Transport properties (D, μ, k,..)
Canonical ensemble	N, V, T	Phase properties (P, H, C_v, μ,…)
Grand Canonical Ensemble	μ_i, V, T	Adsorption isotherms, selectivities
Isothermal-isobaric ensemble	N, P, T	Phase properties (H, C_p, ρ, μ…)
Gibbs ensemble at imposed global volume (m phases)	$N = N_1 + \dots N_m$, $V = V_1 + \dots V_m$, T	Phase equilibrium of pure components and mixtures
Gibbs ensemble at imposed pressure (m phases)	$N = N_1 + \dots N_m$, P, T	Phase equilibrium of mixtures

In the selection of ensemble type, the constraints correspond to the variables that are controlled in the experimental set-up. Unconstrained variables fluctuate and their statistical averages result in predictions, which can be compared with experimental measurements.

In this study, adsorption simulations are analyzed. The ensemble that represents the adsorption in microporous solids is the Grand Canonical Ensemble, which is used in MC method. Detailed explanation is given in the section 3.5.1.

3.2. Molecular Forcefield

The potential energy U involves intermolecular (U_{ext}: external) and intramolecular (U_{int}) energy. Intermolecular energy is the reason of interactions between molecules; it consists of dispersion-repulsion ($U_{d\text{-}r}$) interactions, electrostatic (U_{el}: Coulombic) energy, and polarization (U_{pol}) energy (Equation 3.1-2).

$$U = U_{int} + U_{ext} \quad \textbf{(3.1)}$$

$$U_{ext} = U_{d\text{-}r} + U_{el} + U_{pol} \quad \textbf{(3.2)}$$

The dispersion-repulsion energy is the summation of all pairs of force centers [23].

The potential energy of N interacting particles is given in Equation 3.3.

$$E_{pot} = \sum_i u_1(r_i) + \sum_i \sum_{j>i} u_2(r_i, r_j) + \sum_i \sum_{j>i} \sum_{k>j>i} u_3(r_i, r_j, r_k) + \ldots \quad \textbf{(3.3)}$$

where the first term represents the outer effect. The remaining terms show the particle interactions. For example; u_2 is the interaction between particle pairs, on the other hand u_3 is the interaction between particle trios. The interaction between particle pairs has the larger effect, so the terms after first two terms can be neglected. The most time spending part is the interaction calculations. The simulation algorithm is of N^m degree; by $m \geq 2$, m is the interaction number. Overall, the interactions of groups having three or more particles will cause an increase in calculation time, compared to particle pair interactions. So, an assumption has been made by reducing the fluid interactions to pair interactions.

As mentioned before, intermolecular attraction and repulsion forces have a role on the calculation of the potential energy. The intermolecular interactions are the results of short and long distance effects.

The fluids have a continuous intermolecular potential, which is expressed in Equation 3.4.

$$u(r) = \varepsilon \left[\left(\frac{m}{n-m} \right) x^{-n} - \left(\frac{n}{n-m} \right) x^{-m} \right] \quad \textbf{(3.4)}$$

Here, n and m are constant values; r_m represents the intermolecular distance, which is the result of the minimum energy, x stands for r/r_m . By replacing m and n with 6 and 12 respectively, Lennard-Jones (LJ) potential is obtained (Equation 3.5). It is appropriate to use the LJ potential for neutral, nonpolar molecules [42,43].

$$U_{d\text{-}r} = \sum_{\substack{i,j \\ i<j}} 4\epsilon_{ij} \left(\left(\frac{\sigma_{ij}}{r_{ij}} \right)^{12} - \left(\frac{\sigma_{ij}}{r_{ij}} \right)^{6} \right) \quad \textbf{(3.5)}$$

Here, r, ε, and σ terms indicate the separation distance, LJ well depth, and LJ size, respectively, for the specified pair of groups. i and j represent two different species [26].

Neutral atoms and molecules get affected from two different forces, which are effective at long and short distances. These are the attractive force for long distances and the repulsive force for short distances. LJ potential is mostly used in molecular simulations, because it is a simple and continuous potential to present the intermolecular interactions. LJ potential is a mathematical model that describes the interaction between two neutral atoms or molecules. As it is seen in Figure 3.1, two neutral atoms or molecules pull each other at a certain distance, on the other hand when they get closer they push each other because of the electron cloud [43].

An alternative to LJ is the Buckingham potential (Figure 3.1). It is a model for zeolite short-range interactions between the Na cations and the oxygen atoms of the faujasite (Equation 3.6).

$$V_{Buck} = \sum_{i>j} \left[A_{ij} e^{-r_{ij}/\rho_{ij}} - \frac{C_{ij}}{r_{ij}^{6}} \right] \quad \textbf{(3.6)}$$

The Buckingham potential contains the updated Van der Waals force terms for zeolitic atoms. ρ_{ij} term is the characteristic distance between the atoms denoted by i and j [42,44].

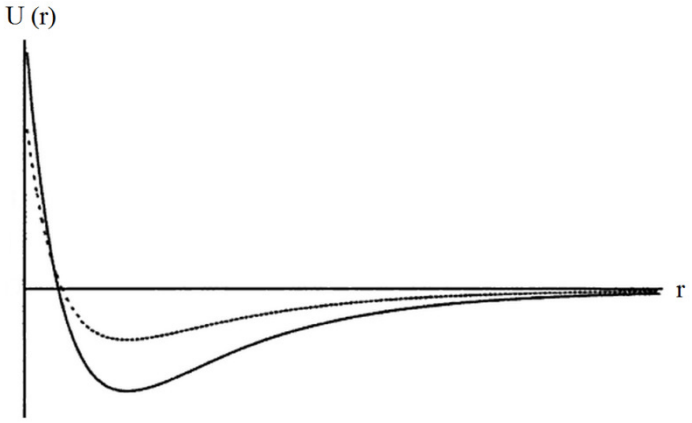

Figure 3.1 : Potential energy plot versus intermolecular distance. The solid curve is LJ, the dashed curve is the Buckingham potential

The calculation of parameters for two species given in Equation 3.7-8 is accomplished by the use of Lorentz-Berthelot combining rule [45].

$$\sigma_{ij}=\frac{\sigma_{ii}+\sigma_{jj}}{2} \tag{3.7}$$

$$\epsilon_{ij}=\sqrt{\epsilon_{ii}.\epsilon_{jj}} \tag{3.8}$$

The force centers of molecules can be defined by three different models: all atoms (AA) in which individual atoms have their own force centers, united atoms (UA) model where a force center represents a group of atoms and is on the main atom of the group, and anisotropic united atoms (AUA) model. In the last model, the force center has a place in the region between the atoms in the group.

The electrostatic energy, which was symbolized by U_{el} earlier, is calculated by Coulomb's law. Here, molecules are assumed to have electrostatic point charges (Equation 3.9).

$$U_{el}=\sum_{\substack{i,j \\ i<j}} \frac{1}{4\pi\varepsilon_0}\frac{q_i q_j}{r_{ij}} \tag{3.9}$$

where q_i and q_j stand for partial charges of species i and j, respectively. r_{ij} is the separation distance and $\varepsilon_0=8.854.10^{-12}$ $C^2N^{-1}m^{-2}$ is the electrostatic constant [26,47]. The polarization energy occurs owing to the electric field and results in a dipole on the particle. For many small molecules, polarization energy can be obtained from experimental measurements [22,47].

The intramolecular energy is classically the sum of four terms (Figure 3.2): stretching energy, which depends on bond lengths, bending energy, which depends on the angle between two bonds, torsion energy, which depends on the dihedral angle, formed by three bonds, and lastly the dispersion-repulsion between distant atoms by which overlaps in a molecule are avoided.

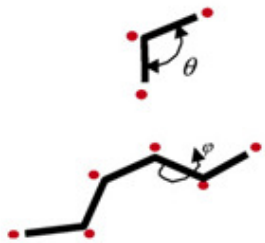

Bending energy (bond angles): $U^{bend} = \frac{1}{2} k_{bend} \left(cos(\theta) cos(\theta_0) \right)^2$

Torsion energy (dihedral angles): $U^{tors} = \sum_{k=0}^{8} a_k cos^k(\varphi)$

Figure 3.2 : Intramolecular energy terms for flexible molecules [22]

During the MC simulation of the thermophysical properties of common fluids, bond lengths are assumed to be constant, so stretching energy is ignored. Consequently, computing time shortens, and it is possible to use longer time steps. It is important to note that intramolecular energy is the sum of aforementioned energies only for flexible molecules. If a molecule is assumed to be rigid, these calculations are totally neglected [22].

3.3. Periodic Boundary Conditions

Periodic boundary conditions (PBC) are applied by drawing an unlimited cage imitating the cubic simulation box. Each of the molecules in the sample box has its images in the other boxes. Each change in each box is applied to the other boxes. If one molecule leaves its box, its image in the neighbor box enters the box from the other side. Consequently, the box in the middle lacks any boundary condition and the surface effects are eliminated [41,47].

By using PBCs, the problem with surface molecules is removed but another problem about the simulations comes out. The most important part of the simulation program is the calculation of the molecular forces and energies. If there are N molecules in the simulation, N-1 terms must be summed in order to calculate the forces and energies of pairs. In principle, it is impossible to add the interactions of the periodic copies into the calculation. This problem is solved by the minimum image convention with the existence of the short distanced intermolecular potential.

In order to calculate the interaction of a molecule with the other molecules, a box that has this molecule in the center is taken. This center molecule interacts with the ones whose center is in this region. If the origin of the coordinate system is accepted as the center of the simulation box with edge length *L*, the algorithms needed for the application of the minimum image rule and PBCs are simplified. All of the coordinates are between *L/2* and *–L/2*. Consequently, when the molecule leaves the box, the copy image is focused on by adding or subtracting *L* to the coordinates [41,47].

The PBCs provide correction of the errors caused by the surface effects, also shortens the calculation time [41,47].

3.4. Ewald Sum

The Ewald sum is used for calculating the contribution of long-term interactions to the potential energy in a system with boundary conditions. In this method, a central simulation box, with a length of *L* is taken. All the positively and negatively charged *N* number of particles are located in this box. The energy occurring from the electrostatic interactions between *N* molecules in this box is calculated with Equation 3.10.

$$E=\frac{1}{2}\sum_{i=1}^{N}\sum_{j=1}^{N}\frac{q_i q_j}{r_{ij}} \qquad \textbf{(3.10)}$$

This central box can have six periodic images at a distance *L* from itself. Then, Equation 3.10 expands to Equation 3.11.

$$E=\frac{1}{2}\sum_{n_{box}=1}^{6}\sum_{i=1}^{N}\sum_{j=1}^{N}\frac{q_i q_j}{\left|r_{ij}+r_{box}\right|} \qquad \textbf{(3.11)}$$

where r_{box} is the distance between the image box and the central box. For each image, five images can be constructed and so on. At the end of this image enlargement process, a sphere of image boxes is formed. So, the following expression is obtained (Equation 3.12):

$$E=\frac{1}{2}\sum_{n_{box}=1}^{\infty}\sum_{i=1}^{N}\sum_{j=1}^{N}\frac{q_i q_j}{\left|r_{ij}+n\right|} \qquad \textbf{(3.13)}$$

Here, $n=n_xL, n_yL, n_zL$ meaning the summation over all lattice points with n_x, n_y, n_z integers. For $i=j$, $n=0$. Equation 3.13 is named by the Ewald Sum, in which total charge of the system is zero [41,47].

3.5. Monte Carlo Method

It is previously explained that MC only takes positions into account; not velocity, momenta. The velocity, and so the kinetic energy are not neglected, but their contribution to the partition function is determined analytically [41,47]. MC method aims to use an appropriate statistical method to generate suitable configurations of the simulated system, in order to conform the probability distribution of the present statistical ensemble [22]. It is based on probabilities. MC is faster than other methods in investigating systems in equilibrium.

The algorithm used in MC has four fundamental terms. These are;

- Random number generator
- Sampling rule
- Probability distribution functions
- Error estimation

It is important to use a reliable random number generator to get a successful result from the MC program. Especially it is because millions of random numbers are used in MC simulations. Unless the numbers are selected in a certain range with random distribution, MC method cannot give an effective result. In fact, it is also impossible to gain random numbers by using an algorithm, because an algorithm gives reproducible and stable results [41].

The best generator is the pseudo number generator. It uses large prime numbers and the *modulo* arithmetic. This generator uses the relation given in Equation 3.13.

$$R_{j+1}=aR_j+c(modm) \qquad \textbf{(3.13)}$$

In this equation, R_j represents the random numbers, which are generated between 0 and $m-1$. a and c are positive constants. This type of a generator is fast, because it necessitates only a few operations. But, after a while it repeats itself. Also, the next random number is determined depending on the present one, which is an unwanted

situation in MC. The most appropriate method for solving this problem is to use several generators together [41].

3.5.1. Monte Carlo and ensemble behavior

Molecular simulation is carried out with defined thermodynamic properties such as chemical potential (μ), volume (V), and temperature (T). These conditions state the ensemble property of the system. For molecular dynamics, this condition is *NVE*. Here, E indicates the kinetic energy. These conditions are accepted because Newton equations satisfy the energy conservation. Though in Monte Carlo, μVT is valid.

In statistical mechanics, the macroscopic properties such as pressure, density represent the time dependent average over all possible quantum states. In order to calculate the properties of a real system, it is appropriate to define an ensemble. An ensemble can be the combination of many systems from different quantum states carrying general macroscopic properties. For example, it is fundamental that each system in the ensemble carries the same temperature, pressure and molecule number values with the represented real system. The ensemble average of a dynamic property (A) can be determined by Equation 3.14.

$$\langle A \rangle = \sum_i A_i p_i \qquad \textbf{(3.14)}$$

Here, A_i is the value of A in i^{th} quantum state, p_i is the observation probability of i^{th} state, and $\langle A \rangle$ is the ensemble average. As time goes to infinity, it is assumed that A converges to its average value. p_i is defined in Equation 3.15.

$$p_i = \frac{e^{-\beta E_i(N,V)}}{Z_{NVT}} \qquad \textbf{(3.15)}$$

In the equation, E shows the energy, β is $1/k_B T$ (k_B: Boltzmann's constant, T: temperature), and Z_{NVT} is the partition function (Equation 3.16).

$$Z_{NVT} = \sum_i e^{-\beta E_i(N,V)} \qquad \textbf{(3.16)}$$

The ensemble that is concerned is the μVT ensemble used in MC method. Combining all expressions, Equation 3.17 is obtained for the average value.

$$\langle A \rangle = \frac{\int A(r^N) exp\left(-\beta E(r^N)\right) dr^N}{\int exp\left(-\beta E(r^N)\right) dr^N} \quad \textbf{(3.17)}$$

MC method is based on the expression given in Equation 3.17, and carries on the simulations with determining the average values for the searched thermodynamic property [47].

3.5.2. Sampling in Monte Carlo method

MC method generates the solution space of the problem by using the random numbers. In simple sampling technique, each point has equal probability. But in this way, also the points yielding to false results are included, so this technique fails. Because each point does not contribute to the solution equally, some have a larger proportion and some have a smaller, so that they can be eliminated without being included. This is why it is advantaged to do sampling in the region where contribution to the solution is the most. This kind of sampling is called "importance sampling". The difference between two types of sampling can be shown in the integral expressions in Equations 3.18-19.

Simple sampling, $I = \frac{1}{N} \sum_{i}^{N} f(x_i)$ **(3.18)**

Importance sampling, $I = \sum_{i}^{N} \frac{f(x_i)}{p(x_i)}$ **(3.19)**

In the equations above, *p* represents the probability and *f* represents the function that is integrated. As shown; in importance sampling, each point contributes the solution with the reverse of the probability. Different from simple sampling, the weight product is taken instead of the average of all points. As a result, MC method operates sampling according to probability distribution functions. In simple sampling, equal distribution function (EDF) which provides choice with equal probability is used. The most important EDF used in statistics is the Gaussian function. Gaussian function is a bell-shaped curve and is expressed in Equation 3.20.

$$f(x) = \frac{e^{-\frac{(x-\mu)^2}{2\sigma^2}}}{\sqrt{2\pi}} \quad \textbf{(3.20)}$$

Here, μ represents the arithmetic average and σ^2 is the variance. Variance is the expected value of the square of the deviation of the distribution from its average. It is expressed in Equation 3.21.

$$\sigma^2 = \frac{1}{N}\sum_i^N \left(x_i - \mu\right)^2 \quad \textbf{(3.21)}$$

Another EDF that is used is Boltzmann's distribution function that is shown in Equation 3.22.

$$\frac{N_i}{N} = e^{-\frac{E_i}{kT}} \quad \textbf{(3.22)}$$

In this equation, N represents the particle number, E is the energy, T is the temperature and k stands for Boltzmann constant (1.38×10^{-23} J/K) [41].

In MC method, the following steps are carried out respectively:

- A random trial configuration is generated initially.
- Changes in energy and other properties are calculated for this trial configuration, and an acceptance criterion is constituted.
- The acceptance criterion is compared to a random number and the trial configuration is either accepted or rejected.

Not all of the states contribute equally to the determination of the property of the system. That is why the states, which provide the most significant contribution, should be selected in order to determine the properties of the system correctly. In this way, simulation accomplishes in a shorter time [41]. This is achieved by the Markov chain. A new case in Markov chain is accepted provided that it is more convenient then the present one. In the simulation of the ensemble, this indicates that it has a lower energy. Markov chain is necessary to determine the properties of the system in a limited time. Its role is to sample the case giving the most meaningful distribution [41,47].

MC simulation operates by determining average thermodynamic properties. Average of a thermodynamic property is shown by $\langle A(r^N)\rangle$. This value is found by the multi integral calculated over N particles (Equation 3.23).

$$\langle A(r^N)\rangle = \int A(r^N)\rho(r^N)dr^N \quad \textbf{(3.23)}$$

Here, $\rho(r^N)$ is the probability distribution function (Equation 3.24), and indicates the probability of being in the r^N position for the molecule. r^N is the position of the N^{th} molecule.

$$\rho(r^N)=\frac{exp[-\beta E(r^N)]}{\int exp[-\beta E(r^N)]dr^N} \quad \textbf{(3.24)}$$

MC method makes many trials over the r^Ns and changes the integrals with summations. So, thermodynamic average gets its last form as shown in Equation 3.25.

$$\langle A(r^N)\rangle=\frac{\sum_{i=1}^{N_{trial}} A_i(r^N)\, exp[-\beta E_i(r^N)]}{\sum_{i=1}^{N_{trial}} exp[-\beta E_i(r^N)]} \quad \textbf{(3.25)}$$

This type of configuration is not enough to obtain a correct result. Metropolis algorithm is used to complete this insufficiency [41,47].

3.5.3. Metropolis algorithm

The limitations of the random sampling are removed by developing structures which have more contribution to the thermodynamic average. For this purpose, Metropolis sampling is used.

In Metropolis sampling, cases with the probability $e^{-\beta E(r^N)}$ are generated and all are accepted to be equal. In other words, in MC integration, cases with equal probability are generated and weight of $e^{-\beta E(r^N)}$ is assigned to each. The Markov chain produced in Metropolis sampling provides the following conditions:

- The outcome of each trial is only related to the proceeding trial.
- Each trail can produce a series of finite possible outcomes.

The first condition explains the difference between MC and MD simulations clearly. In MD simulations, all the cases depend on time [41,47].

The Metropolis algorithm makes a comparison between sequent states. It accepts or rejects the new state in accordance with Equation 3.26.

$$P_{acc}(old\rightarrow new)=\min\left(1,\frac{\rho_{new}}{\rho_{old}}\right) \quad \textbf{(3.26)}$$

where, ρ is the probability density of the configuration, and P_{acc} is the acceptance probability of that configuration. In order to explain how the algorithm works, NVT ensemble can be taken as an example: For this ensemble, the probability expression is given in Equation 3.27.

$$P_{acc}(old \rightarrow new) = \min\left(1, exp\left(-\beta(U_{new}-U_{old})\right)\right) \quad \textbf{(3.27)}$$

- If $exp\left(-\beta(U_{new}-U_{old})\right) > 1$, which means if $U_{new} < U_{old}$, the new configuration is accepted and is added to the ensemble;
- If $exp\left(-\beta(U_{new}-U_{old})\right) < 1$, which means if $U_{new} > U_{old}$, a random number is selected between 0 and 1 denoted by q, and in that case if $exp\left(-\beta(U_{new}-U_{old})\right) > q$, the new configuration is accepted and added to the ensemble. Otherwise the new one is rejected, and the old one is accepted [41,48].

In MC method, there are different types of MC moves (Figure 3.3). These are explained in the following title.

3.5.4. Monte Carlo moves

Translation is one of the MC moves in which individual molecule displays a translation. This procedure follows as:

- A translation vector having random components is defined, and a random molecule selection is made.
- The translation vector is applied to the atoms of this molecule, and a new test configuration is obtained.
- The potential energy of this configuration is calculated.
- The acceptance criterion given in Equation 3.26 is applied.

By translation, no change occurs in the internal conformation of the molecule. The components of translation vector cannot exceed the dimensions of the simulation box.

Translation move is limited with monatomic molecules in the NVT ensemble. For other molecules and ensembles, different moves are needed [41].

In the rotational MC move, a random direction and a random angle are selected and the molecule moves according to them. The angle is chosen from a limited interval, which provides acceptance for the configuration. In this move, the molecule is accepted as a rigid body, which means torsion, bending and bond effects are conserved. The acceptance criterion (Equation 3.26) is applied [41].

In order to avoid volume fluctuations, volume exchange is applied by which the simulation box either expands or shrinks. Again, the volume difference ΔV is selected randomly from a limited interval. In this MC move, molecule mass centers do not change and each molecule is translated with varying translation vectors. The acceptance criterion for NPT ensemble applied in this move is given in Equation 3.28.

$$P_{acc}(old \rightarrow new) = \min\left(1, \left(\frac{V+\Delta V}{V}\right)^{N} exp\left(-\beta\left(U^{new} - U^{old} + P\Delta V\right)\right)\right) \quad \textbf{(3.28)}$$

Here, P is the pressure, V is the volume, and N is the number of molecules in the simulation box [41,48].

In displacement move, a molecule is selected randomly, and is deleted. Then, it is located in the simulation box randomly. In partial regrowth move, one end of the molecule is cut and it is allowed to regrow at a random position. These moves are usually applied together with configurational bias. However, in this study, large molecules are not used. That is why only Metropolis algorithm is in the scope of this study [41,48].

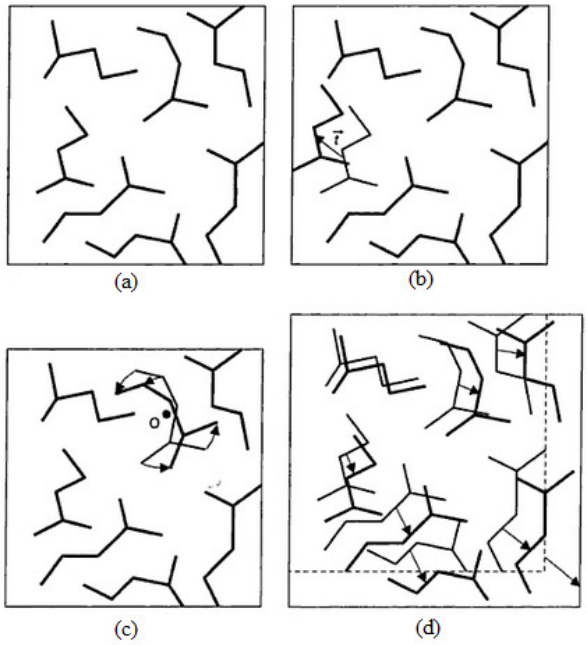

Figure 3.3 : General MC moves. (a) initial configuration (b) translation (c) rotation (d) volume exchange [48]

The simulations are performed inside cubic cages where there are hundreds of molecules. As long as the sample box is small in size, most of the molecules lie upon the surface of the cage rather than in the bulk. This is an undesired situation because the forces in the bulk and on the surface differ. PBCs are used in order to avoid this problem [48].

3.5.5. Averages and error estimations

Averages in MC simulation are determined after the equilibration process. Number of steps needed for the equilibration is not known formerly, it must be obtained from trial simulations.

The deviation from the average value found in the loops after equilibrium step is the error. If the error estimation is large, this can have two reasons:

- Simulation has started without reaching equilibrium.
- For some reason, simulation is not reliable.

The average value of a property is given in Equation 3.29.

$$\langle A \rangle_{run} = \frac{1}{N\text{-}N_{equil}\text{-}1} \sum_{i>N_{equil}}^{N} A_i \qquad \textbf{(3.29)}$$

Here, $\langle A \rangle_{run}$ is the average value, N is the loop number. N_{equil} shows the loop number needed to reach equilibrium. The process after equilibrium is separated to N_b blocks with length of l. For each block, the average value of A is found as it is given in Equation 3.30.

$$\langle A \rangle_b = \frac{1}{l} \sum_{i=1}^{n_b} A_i \qquad \textbf{(3.30)}$$

The standard deviation (σ) is obtained from the average of all blocks (Equation 3.31).

$$\sigma = \sqrt{\frac{1}{n_b} \sum_{b=1}^{n_b} (\langle A \rangle_b - \langle A \rangle_{run})^2} \qquad \textbf{(3.31)}$$

The magnitude of the error is associated with the quality of the simulation. The smaller the standard deviation is, the higher the quality of the simulation is [41].

3.6. Molecular Dynamics Method

Molecular dynamics (MD) method does not depend on probabilities as Monte Carlo (MC) does. It is deterministic, not stochastic. In order to obtain new configurations, it integrates Newton's equations of motion for N particles, and gives results about the time-dependent properties of the system used. It can use different types of algorithms to solve the equations. The force calculation needs longer time than other operations, so compared to MC, MD proceeds more slowly. It is important to shorten the simulation time. For the solution of equations of motion, a finite difference algorithm must be used. It can be either predictor or predictor-corrector method. In the predictor method, the coordinates of the molecules are obtained from current quantities or from previous steps. The mostly used algorithm for this type is the Verlet algorithm (1967) and its modifications. In the predictor-corrector method, different from the predictor method, the coordinates of the molecules are predicted and this data is used to calculate a function particular to the algorithm. Then, the result is used to correct the initial prediction. The Gear algorithm (1971) is the most widely used algorithm for this type [26,41].

3.6.1. Integrating the equations of motion

Before giving detailed explanations about the algorithms used in MD, it is important to know about the motion of the particles in the system. The force on a moving particle is shown in Equation 3.32 where *m* is the mass, *a* is the acceleration, and *F* is the force on the particle.

$$F_i=m_i a_i \tag{3.32}$$

This expression can be converted to an equation including terms depending on time (Equation 3.33), because as mentioned before, MD method depends on time.

$$\frac{d^2 r_i}{dt^2}=\frac{F_i}{m_i} \tag{3.33}$$

Here, *r* represents the position of the particle. This equation is the basis of dynamic behavior. By integration depending on time (Equation 3.34), applying the initial condition (Equation 3.35), ($v=v_i$ at $t=0$, where *v* is the velocity), and once again integrating with respect to time, Equation 3.36 is obtained,

$$\frac{dr_i}{dt}=\left(\frac{F_i}{m_i}\right)t+c_1 \tag{3.34}$$

$$c_1=v_i \tag{3.35}$$

$$r_i=v_i t+\frac{a_i t^2}{2}+c_2 \tag{3.36}$$

where c_2 is the initial position of the particle. By Equation 3.37, it is possible to calculate the displacement of the particle only with its initial velocity and acceleration [41].

3.6.2. Verlet algorithm

Verlet algorithm is originally based on Taylor series expansion (Equation 3.38-9):

$$r(t+\Delta t)=r(t)+\frac{dr}{dt}\Delta t+\frac{1}{2!}\frac{d^2 r}{dt^2}\Delta t^2+\ldots \tag{3.38}$$

$$r(t-\Delta t)=r(t)-\frac{dr}{dt}\Delta t+\frac{1}{2!}\frac{d^2 r}{dt^2}\Delta t^2-\ldots \tag{3.39}$$

The combination of these equations gives the Verlet algorithm (Equation 3.39):

$$r(t+\Delta t)=2r(t)-r(t-\Delta t)+\frac{d^2r}{dt^2}\Delta t^2 \quad \textbf{(3.39)}$$

The advantage of the Verlet algorithm is that it allows determination of the molecular positions without velocity calculation. However, velocities are necessary for kinetic energy calculation. Equation 3.40 gives velocity values.

$$v(t)=\frac{r(t+\Delta t)-r(t-\Delta t)}{2\Delta t} \quad \textbf{(3.40)}$$

The Verlet algorithm is time reversible, and this is an advantage that it conserves energy for long time steps. However, it cannot start by itself. For the calculations at $t=0$, an estimation should be made for the position at $t=-\Delta t$. In addition, as it is obvious in Equation 3.40 that the velocity values are one step behind the coordinates. In order to take these insufficiencies away, modifications are applied to the algorithm. The other integration algorithms are the Leap-frog Verlet Algorithm (1970) and the Velocity Verlet Algorithm. Leap-frog Algorithm provides velocity calculations at half time intervals resulting in new position calculations. However, still velocity and positions are not defined simultaneously. Velocity Verlet Algorithm makes it possible to calculate both velocity and the position at the same time (Equation 3.41-43) [41,48].

$$r(t+\Delta t)=r(t)+v(t)\Delta t+\frac{a(t)\Delta t^2}{2} \quad \textbf{(3.41)}$$

$$v(t+\Delta t/2)=v(t)+\frac{a(t)\Delta t}{2} \quad \textbf{(3.42)}$$

$$v(t+\Delta t)=v(t+\Delta t/2)+\frac{a(t+\Delta t)\Delta t}{2} \quad \textbf{(3.43)}$$

3.6.3. Molecular dynamics and ensemble behavior

In MD, microcanonical (*NVE*) ensemble is default, because energy is conserved by Newton's equations of motion. The number of particles, volume, and energy are the constant constraints. Using this ensemble, firstly initial velocities are assigned to the atoms, whether randomly or set to zero, because they are already corrected in the integrator. Then, the initial forces are calculated over $N(N-1)$ interactions. Meanwhile, accelerations are calculated from Equation 3.32. Total potential energy is also calculated while forces are evaluated. The new forces are used to evaluate

Newton's equations of motion, and to obtain new coordinates, velocities, and other time dependent terms for the atoms [41].

As mentioned before, number of particles, volume, and energy are constant in microcanonical ensemble. N and V are selected constant during initialization, and they do not fluctuate because they are not involved in the simulation algorithm. However, the total energy is to be controlled, via the kinetic energy. In the beginning of the simulation, a desired energy for particles is selected. Then, by the calculation of the potential energy, the kinetic energy is obtained from the substitution of the calculated potential energy from the desired total energy value. The desired energy can be obtained by assigning the necessary initial velocity value according to Equation 3.44,

$$v_i^{new} = v_i \sqrt{\frac{K_D}{K_A}} \tag{3.44}$$

where K_D and K_A are the desired and actual kinetic energies, respectively. By this way, energy fluctuations are avoided. However, a drift in energy may be observed depending on the inaccuracies in force calculations. So, only during the equilibration process, velocities are periodically scaled [41].

In order to use temperature information, canonical ensemble (Table 3.1) is used. In this ensemble, different from the microcanonical, temperature is constant instead of energy. There are different methods for generating canonical ensemble. Velocity scaling and heath-bath coupling are the simplest ones. Besides; Andersen (1980), Nosé (1984), Hoover (1985) thermostats, and the general constraint (Hoover et al., 1984; Evans, 1983) are the other methods. The latter ones apply modifications to the equations of motion.

In Andersen thermostat, velocity scaling is performed by combining stochastic processes and molecular dynamics, and so canonical distribution is obtained. On the other hand, in Nosé thermostat, there is a thermal reservoir in the integral part of the system that denotes an additional degree of freedom. Hoover has reorganized Nosé's equations of motion, and has removed the extra degree of freedom [41].

3.6.4. Diffusion coefficient

In this study, MD method is applied for diffusion calculations. The self-diffusion coefficient is obtained from the following equation (Equation 3.45).

$$D=\lim_{t\to\infty}\frac{1}{2kNt}\left\langle\sum_{j=1}^{N}\left|r_j(t)-r_j(0)\right|^2\right\rangle \quad \textbf{(3.45)}$$

Here, D shows the diffusion coefficient, N is the number of particles, r is the position, $k=1,2,$ *or* 3 depending of the dimension of the system, and t is time. $\langle|r_j(t)-r_j(0)|^2\rangle$ is the mean square displacement (MSD) of the ensemble. This equation can be reduced to Equation 3.46 [41,48].

$$\langle r^2(t)\rangle=2kDt \quad \textbf{(3.46)}$$

4. ADSORPTION SIMULATIONS

Molecular simulations have an important place in adsorption, diffusion, and the synthesis of zeolitic materials. Twenty years ago, it was not possible to perform adsorption simulations except for noble gases or small alkane in purely siliceous zeolites. Today, scientists are able to simulate large chain alkane, aromatic molecules and other fluids in many cationic zeolites [43].

Simulations covered in this study are performed using two softwares: *Gibbs*, which is written in *Fortran 90* code, computes the phase equilibria properties of fluids by molecular simulation, using the MC method. MTBE adsorptions are carried out by using *Gibbs*, on the other hand *Materials Studio 4.1* is used for TCE adsorption and for all diffusion simulations. *Materials Studio 4.1* is a software that provides sampling and simulation solutions for studying chemicals and materials such as crystal structure and crystallization processes, polymer properties, catalyze and structure-activity relations [47,52].

There are various forcefield types in the software *Materials Studio 4.1*. In this study, CVFF (Consistent-Valence Force Field) is used, and is modified according to the characteristics of the studied system. Generally, CVFF is configured for amino acids, water and various functional groups. Besides, it contains additional atom types for aluminosilicates and aluminophosphates. It is suitable for small organic crystals and gas phased structures. It comprises peptides, proteins, and organic systems. Basically, CVFF studies the structures and their binding energy, but it can also make reasonable predictions about vibrational frequencies and conformational energies [52].

The adsorption experiments can give detailed information about the macroscopic properties of the process, but it is important to learn the atomic details to know about microscopic behavior. So, molecular simulation techniques such as MC complete these missing parts of the experiments [53,54].

4.1. Faujasite Structure

Faujasite (FAU) is a natural high-porosity zeolite having different Si/Al ratios. Its name represents a topology. Zeolite X, Y, and USY (Ultra-Stable-Y) are types of it. It consists of sodalite or in other words β-cage units, which are shown in Figure 4.1.

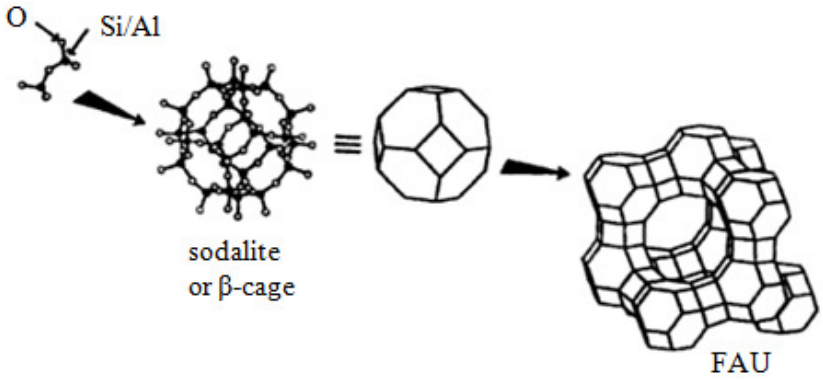

Figure 4.1 : Faujasite structure

In Figure 4.1, it is obvious that a pair of TO_4 tetrahedra is linked to a single sodalite cage by T-O-T bonds. In the FAU zeolite representation, oxygen atoms are not shown; instead, tetrahedral (T) atoms are connected via straight lines. In faujasite, there are pores containing 12-membered rings with an approximate diameter of 7.6Å. The larger the pore is, the easier movement is provided for the guest molecules. The unit cell parameters of FAU zeolite are 25.028Å in three axes [25].

4.2. ZSM-5 Structure

ZSM-5 zeolite is in MFI structure. It is composed of 96 SiO_2 units. ZSM-5 zeolite structure has two types of channels containing 10-membered rings: elliptical straight channels (SC) with diameter 5.1 x 5.5Å along the y-axis, and the zigzag (or sinusoidal) channels (ZC) with diameter 5.3 x 5.6Å parallel to the xz plane, and also there are intersections (I) of these channels. These are four SC, ZC, and I per unit cell [24,53,54]. The unit cell dimensions for ZSM-5 are a=20.022Å, b=19.899Å, and c=13.383Å, in x, y, and z axes, respectively. In Figure 4.2, an example ZSM-5 type zeolite from different views can be seen. The yellow, red, pink, and purple atoms represent the silicalite, oxygen, aluminum, and sodium atoms, respectively.

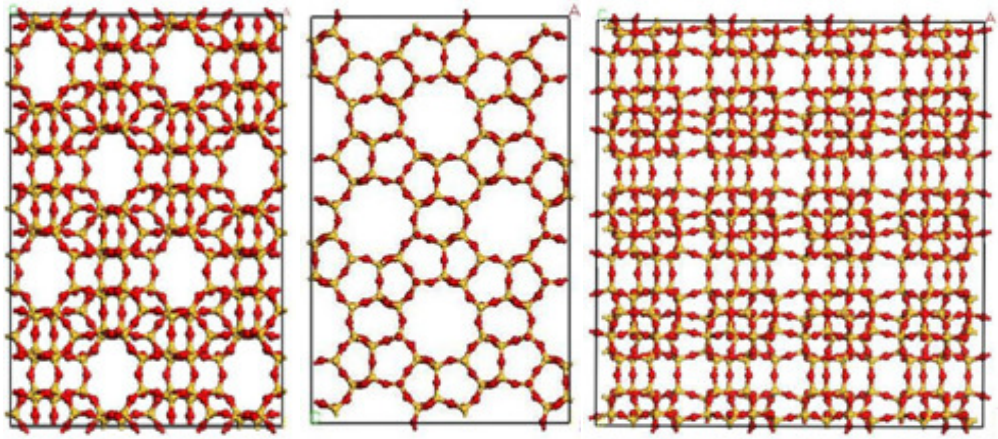

(a) **(b)** **(c)**

Figure 4.2 : A silicalite super cell composed of eight (2×2×2) unit cells along the (a) x-direction (b) y-direction (c) z-direction

The all silica version of ZSM-5 zeolite is called silicalite. It has high thermal and chemical stability, and is highly hydrophobic due to the lack of aluminum atoms and so extra-framework cations. These properties make silicalite suitable for the removal of organics such as chlorinated VOCs from water [30].

4.3. Simulation Method

MTBE adsorption is simulated in Y type faujasites and for TCE adsorptions, ZSM-5 type zeolites are studied additionally. Four FAU zeolites with different Si/Al ratios are used. These are dealuminated Y zeolite (DAY) which contains no aluminum atoms; NaY48, NaY64, and NaY96. In the last three abbreviations, NaY indicates Y type zeolite containing Na^+ cations needed for charge neutralization. The numbers refer to the quantity of cations in the structure.

For TCE adsorption simulations, three different ZSM-5 zeolites with different Si/Al ratios are used. These are silicalite, which contains no aluminum atoms, NaZSM-5 (191), and NaZSM-5 (95). Similar to faujasite naming; in the last two abbreviations, NaZSM-5 indicates ZSM-5 type zeolite containing Na^+ cations needed for charge neutralization. The numbers in parenthesis show the Si/Al ratio. The properties for zeolites used in adsorption simulations are given in Table 4.1.

Table 4.1 : Properties for zeolites used in adsorption simulations

Zeolite Type	Si / Al	Cation number / unit cell	Partial charges (e)				
			T		O		Na^+
			Si	Al	O-Si	O-Al	
Silicalite	∞	0	2.000	-	-1.000	-	-
NaZSM-5 (191)	191	1	2.000	1.700	-1.000	-1.175	1.000
NaZSM-5 (95)	95	2	2.000	1.700	-1.000	-1.175	1.000
DAY	∞	0	2.000		-1.000		-
NaY48 [55]	3	48	1.396		-0.823		1.000
NaY64 [55]	2	64	1.331		-0.832		1.000
NaY96 [55]	1	96	1.200		-0.850		1.000

MTBE adsorption simulations are performed using *Gibbs* software. Al locations are selected randomly and Na^+ cations are inserted via MC simulations. After loading the cations, grid files are created using *Gibbs* software to obtain the coordinates of all atoms in the framework, including the locations of the cations. The distance between grid points is 0.2Å in three-dimensions. The LJ parameters for atoms used in the simulations are given in Table 4.2. All other LJ parameters are obtained from the Lorentz-Berthelot combination rules, which are given in Section 3.2. MTBE is taken as a flexible molecule that is why torsion and bending energies cannot be ignored. The AUA LJ parameters (Table 4.2) are taken from a previous study on optimization of forcefield of ethers by Güvenç [56]. Water molecules are modeled according the Buckingham SPC model developed by Errignton and Panagiotopoulos [57].

Table 4.2 : LJ parameters and elementary charges of atoms used in the adsorption simulations

Atom type	LJ parameters		**q (e)**
	σ (Å)	**ε/k_B (K)**	
O (zeolite) [6,7]	3.00	93.53	given in Table 4.1
CH_3 (MTBE) [56]	3.6072	120.15	0.185726785
CH_3 (MTBE) (CH_3-C)[56]	3.6072	126.2264	0
C (MTBE) [56]	3.345	4.9529	0.185726785
O (MTBE) [56]	2.991	59.69	-0.37145357
C (TCE)	3.8231	88.93	-0.064, 0.036 [11]
Cl (TCE)	3.7782	60.753	-0.068, -0.022, -0.054 [11]
H (TCE)	3.1681	45.042	0.172 [11]
O (water)	3.586	130.278	0.7374
H (water)	-	-	-0.3687
Na [58]	2.584	50.34	1.000

GCMC ensemble is used for MTBE adsorption simulations. Ewald summation method is used for the correction of long-range electrostatic interactions. The cut-off distance is set to half of the minimum box size.

MTBE simulations are performed under 298K, 323K, and 348K. Isotherms are calculated at 22 pressure points within the logarithmically scaled interval of 10^{-6}-10^{5}kPa with 5 million steps for each point. Comparisons are made with respect to zeolite structure and temperature.

Simulations of TCE adsorptions in faujasites are performed using *Materials Studio 4.1* software, using CVFF with a modification in LJ parameters. FAU zeolite structure is taken from the software library, TCE molecule is taken from the study of Mellot *et al.* [10] (Table 4.2). *Sorption* module is used for adsorption simulations. 1 million steps are applied for both equilibrium and production steps. Isotherms are calculated within the interval 10^{-3}-2kPa over 21 points. Temperature is set to 298K for these simulations.

In addition to simulations of TCE adsorption in FAU zeolites, both aqueous and pure TCE adsorptions are carried out in ZSM-5 type zeolites. The properties of the water model used here are given in Table 4.2.

4.4. Results and Discussions

Adsorption isotherms of MTBE in faujasites with respect to temperature and zeolite structure are illustrated in Figures 4.3-4. As seen in Figures 4.3, saturation capacity for MTBE adsorption is around approximately 30 molecules/unit cell of zeolite. This means that extraframework cations do not affect the maximum loading capacity. Adsorption isotherm is sharper in high aluminum existence, in contrast to DAY that contains no aluminum, theoretically: The sequence is as NaY48 > NaY64 > NaY96 > DAY. Thus, extraframework cations have more significant effect on loadings at low pressures. Temperature effect is seen in Figure 4.4. As expected, loading steepness decreases as temperature increases, because stronger intermolecular attractions occur at low temperatures, and adsorption capacity decreases at lower pressures.

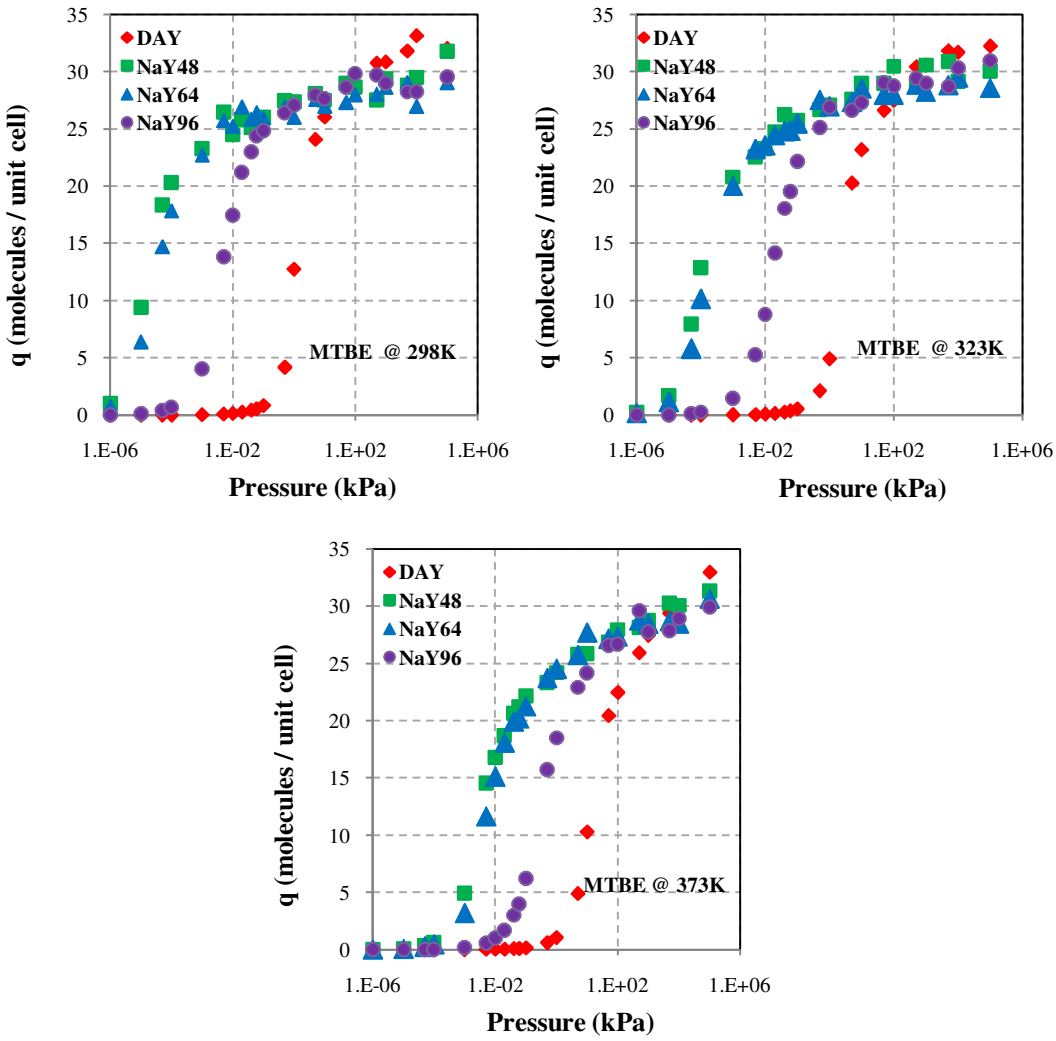

Figure 4.3 : Adsorption isotherms of MTBE with respect to temperature

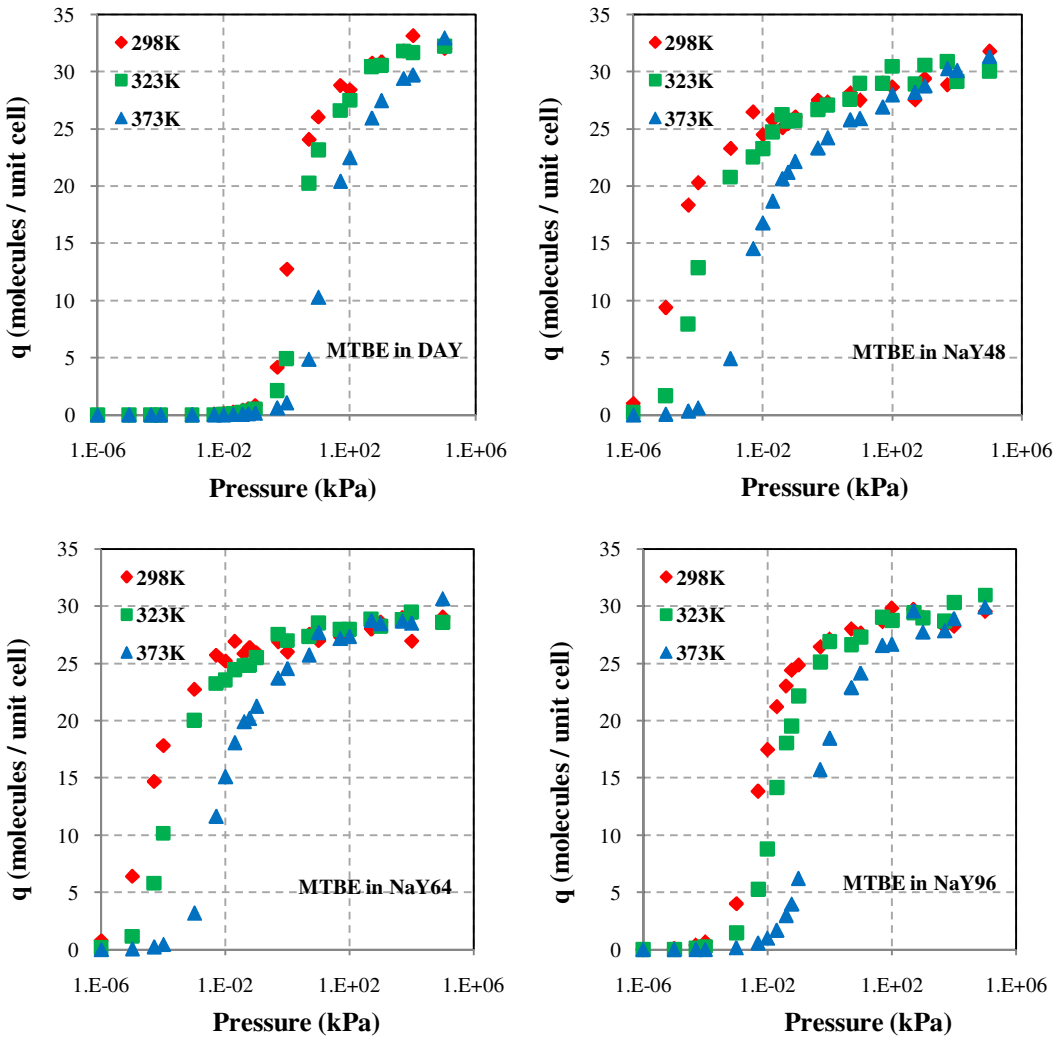

Figure 4.4 : Adsorption isotherms of MTBE with respect to zeolite structure

Pure TCE adsorption isotherms in faujasites are given in Figures 4.5-6. Comparisons with past experimental studies performed by Clausse *et al.* [26,28] and Giaya *et al.* [30] are also included. PCFF [39] and COMPASS [59] forcefields are also tested for TCE adsorption simulations, but it is found that CVFF is the most consistent one with the previous works (Figure 4.6). So, this simulation study is proved to be conforming to experimental measurements. It is also clear that TCE in DAY has a saturation value around 26 molecules per unit cell. This value is around 40 molecules/unit cell for aluminum containing structures. The loading increase is so steep in NaY zeolites between 0-0.1kPa that it cannot be observed (Figure 4.5).

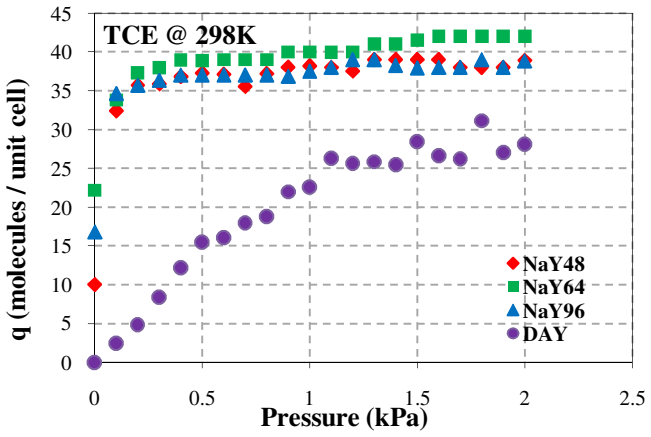

Figure 4.5 : Adsorption isotherms of TCE in faujasites

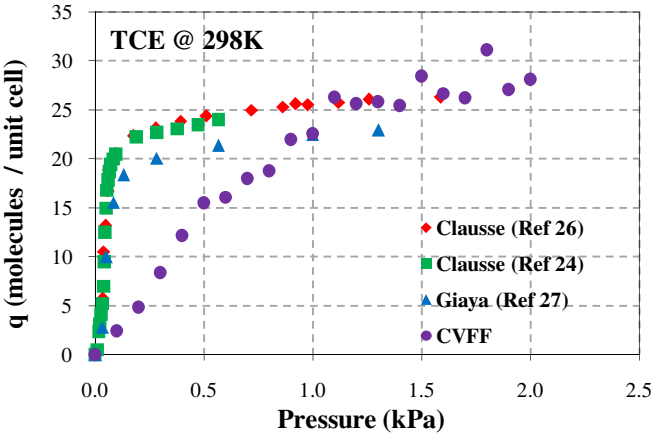

Figure 4.6 : Adsorption isotherms of TCE in DAY

Next, concentration profiles of TCE molecules adsorbed in FAUs are calculated as given in Figure 4.7. It is observed that in all structures, TCE molecules are homogeneously adsorbed into the pores formed by the β-cages.

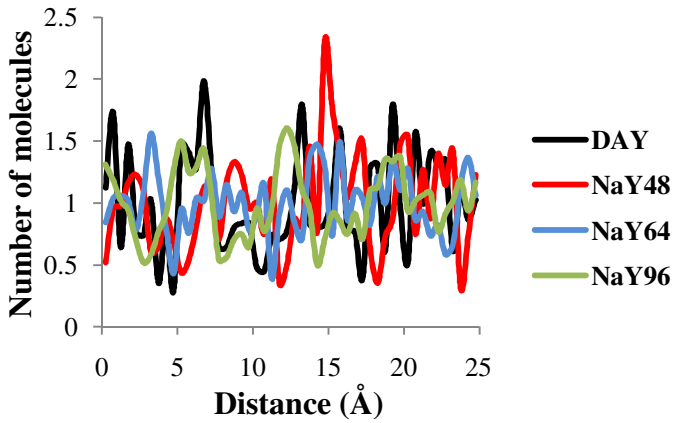

Figure 4.7 : Concentration profiles of TCE in faujasites

In Figure 4.8, both TCE and water adsorptions in ZSM-5 are shown. According to the isotherms, pure TCE saturation of ZSM-5 zeolite is obtained around 9 molecules per unit cell. In addition, simulations conform to the experimental study of Giaya *et al.* [30].

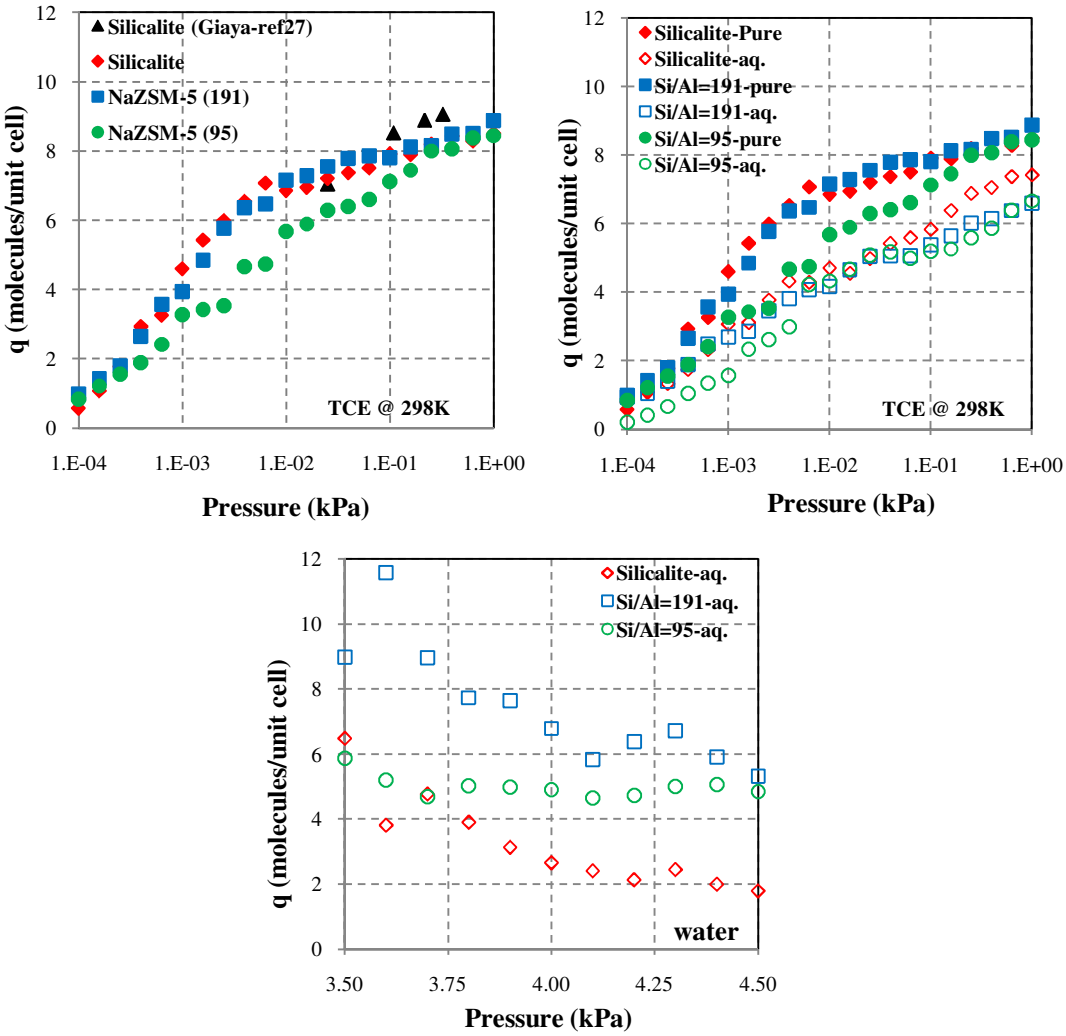

Figure 4.8 : Adsorption isotherms of TCE and water in ZSM-5

Loadings increase steeply in the presence of lower cation number. Unlike MTBE simulations, cations have negative effect on the characteristics of TCE adsorption isotherms. This behavior is valid for both pure and aqueous adsorptions. It is obvious that for aqueous ones, TCE loading increases as water amount decreases. This means that TCE takes place of water molecules in the pores of the structure with rising pressure. For water adsorptions, loading sequence is as the following: Silicalite<NaZSM-5(95)<NaZSM-5(191) which does not represent a regular increase with respect to increasing cation amount, it is not possible to observe a regular trend. This might be because of the locations of the Al atoms in the zeolite framework.

Concentration profiles of TCE molecules in ZSM-5 structure are plotted along z-direction, in Figure 4.9. Fixed loading simulations are carried out using MC method in NPT ensemble with loading values given in Table 4.3. It is observed that Na^+ cations are present in the intersections of the straight and sinusoidal channels. TCE molecules mostly populate the straight channels and the intersections, for all structures. Water effect is not found to be significant.

Table 4.3 : Number of TCE and water molecules adsorbed in ZSM-5 zeolites

Zeolite type	**Number of TCE molecules per unit cell**		**Number of water molecules per unit cell**
	pure	aqueous	
Silicalite	8	7	1
NaZSM-5 (191)	8	7	6
NaZSM-5 (95)	8	7	4

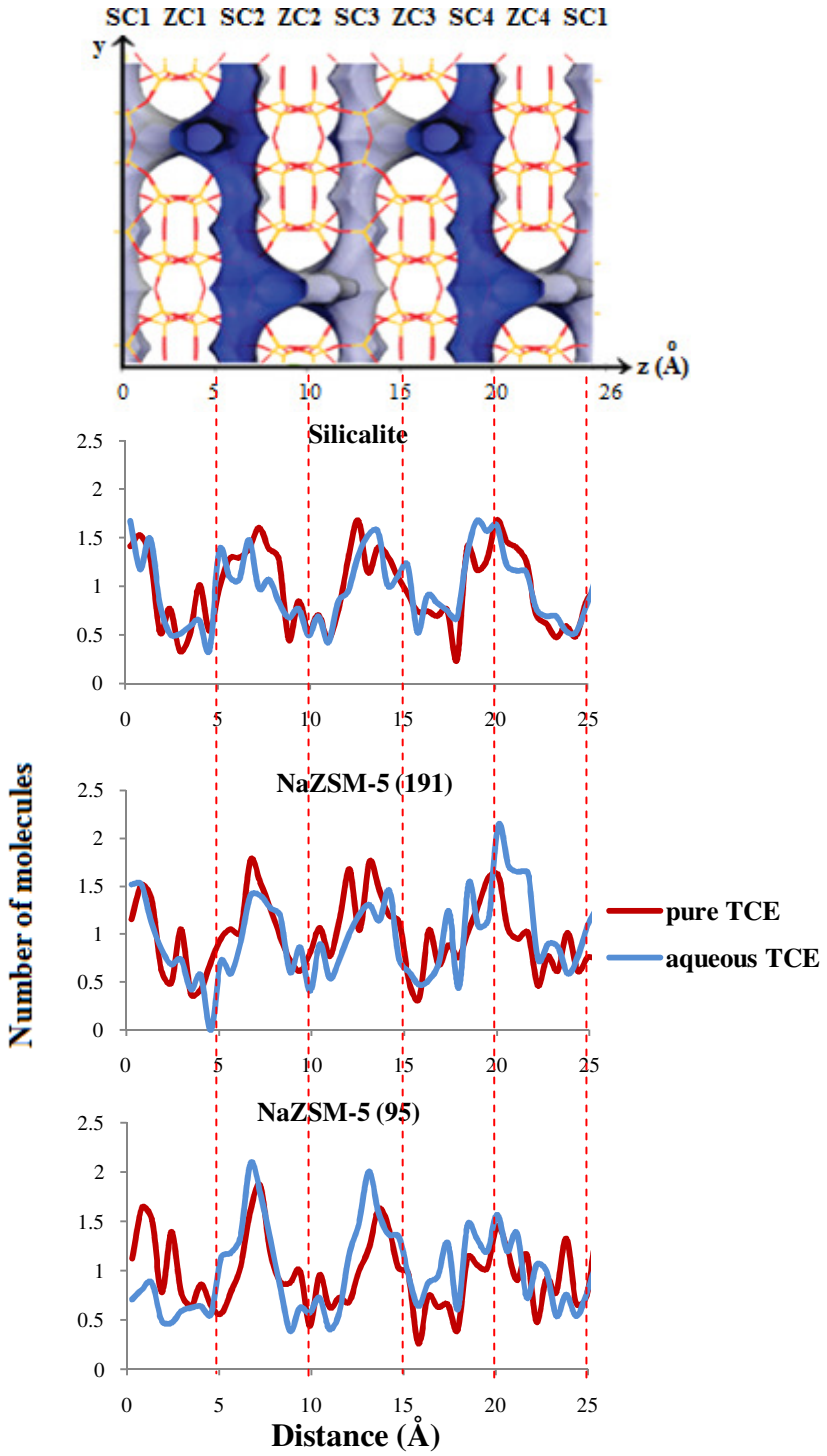

Figure 4.9 : Concentration profiles of TCE adsorbed in ZSM-5 zeolites, with respect to adsorbed TCE, aligned by the projection of ZSM-5 zeolite on yz-plane

In Figure 4.10 it is also seen that aluminum presence does not affect the adsorption behavior. Between 11-17Å in z-direction of silicalite structure, no water molecules are adsorbed. This indicates that water molecules form clusters where they populate which behavior is not observed in NaZSM-5 zeolites owing to cation presence. Besides, water molecules mostly populate around the Al atoms. (Figure 4.11).

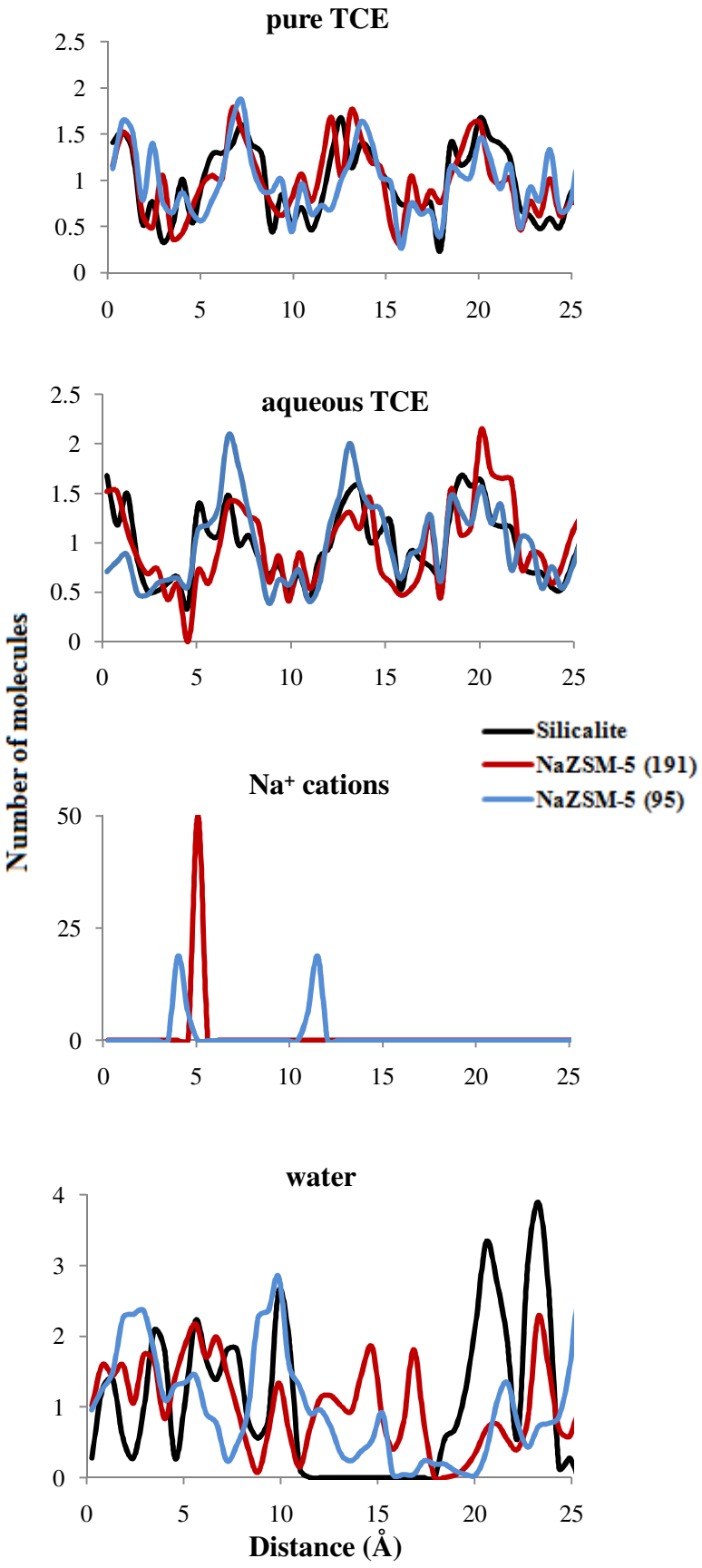

Figure 4.10 : Concentration profiles of molecules and cations in ZSM-5 zeolites with respect to zeolite type

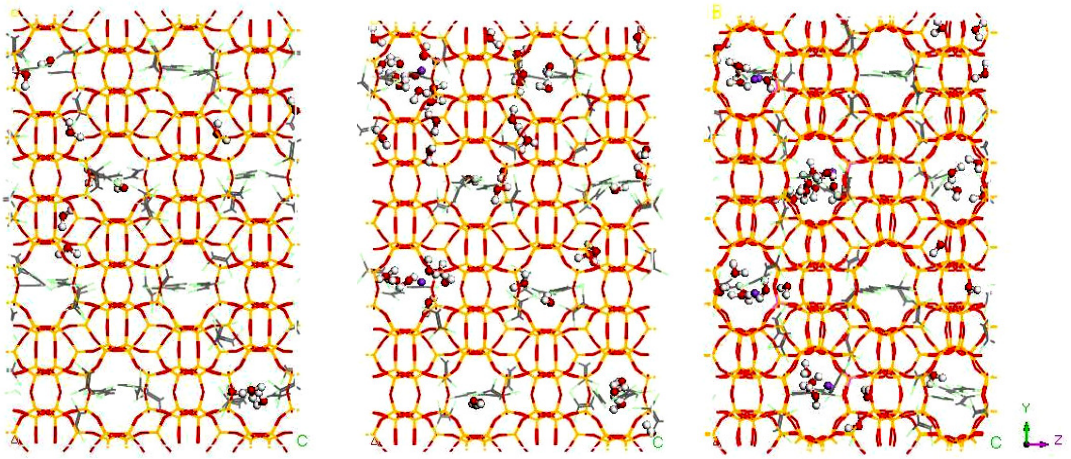

(a) (b) (c)

Figure 4.11 : Snapshot pictures from the simulation box of ZSM-5 - TCE - water system. (a) silicalite (b) NaZSM-5 (191) (c) NaZSM-5 (95)

The radial distribution functions (RDFs) in Figure 4.12 show that TCE molecules do not display an ordered structure in ZSM-5 zeolites. It is observed that the oxygen atoms of water molecules interact with the oxygen atom of the zeolite in shorter distances in the absence of cations (Figure 4.13).

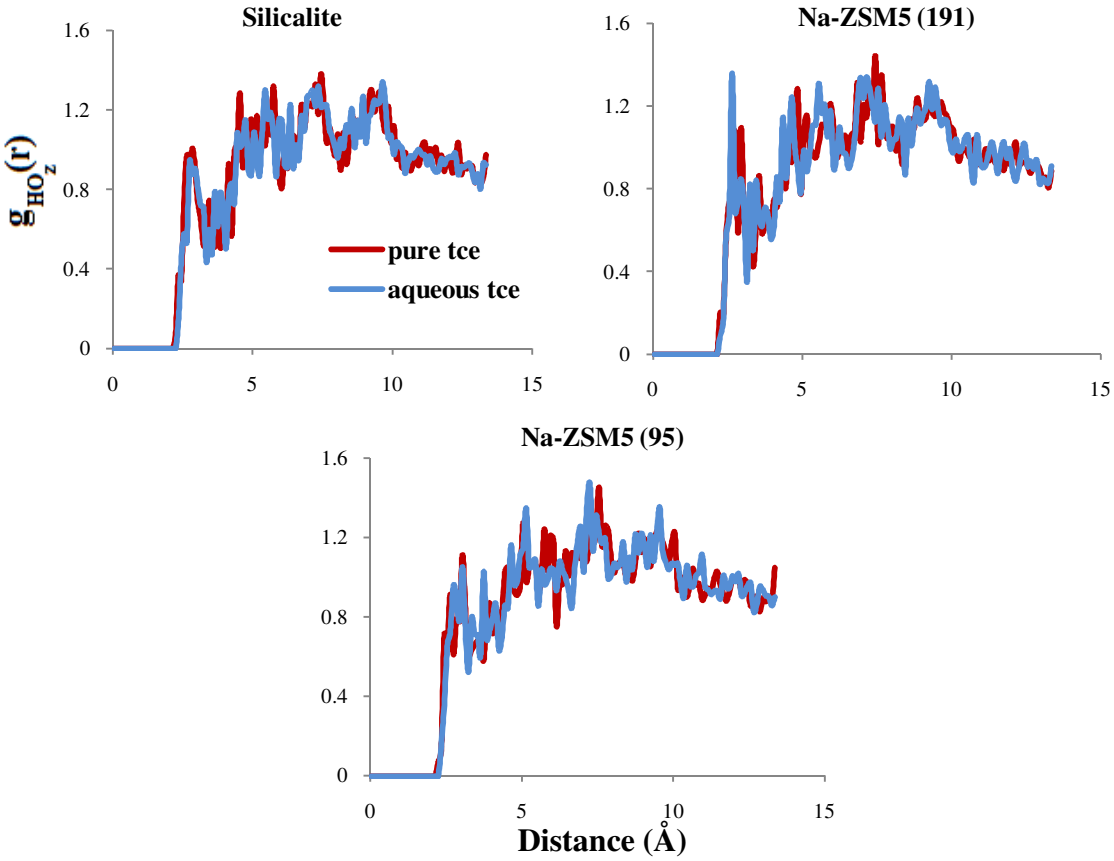

Figure 4.12 : Change in RDFs of hydrogen atoms in TCE molecules with alumina content

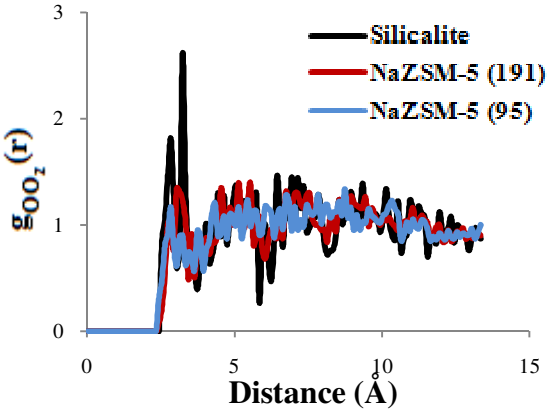

Figure 4.13 : Change in RDFs of oxygen atoms in water molecules with alumina content

In this study, aluminum atoms are located randomly on the zeolite structure; only on the 10-membered rings along the sinusoidal (zigzag) channels as shown in Figure 4.14. Loading properties are not analyzed depending on Al locations. However, one sample simulation is performed for aqueous TCE in NaZSM-5 (95) with Al atoms on both straight (SC) and zigzag channels (ZC) (Figure 4.15). In this simulation, loading calculation could not be completed up to 4.5kPa, and it failed at 3.66kPa.

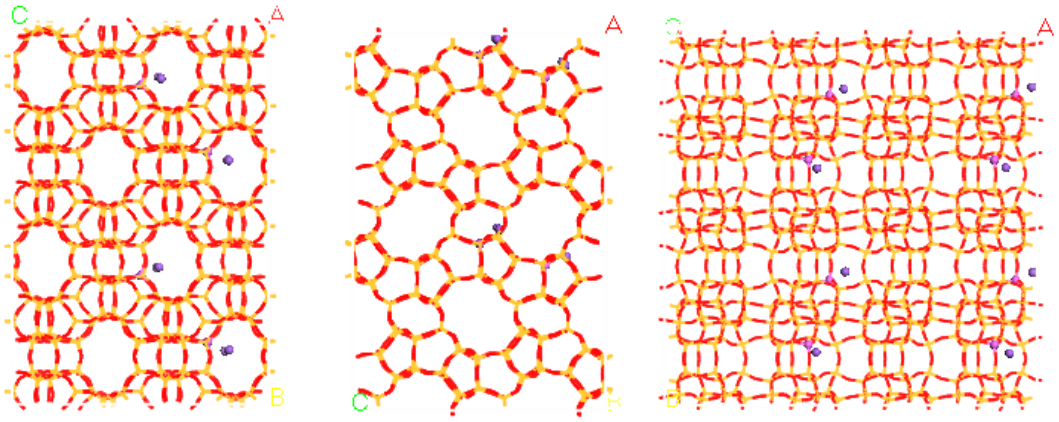

(a) **(b)** **(c)**

Figure 4.14 : A NaZSM-5 (95) composed of eight (2×2×2) unit cells along the (a) x-direction (b) y-direction (c) z-direction, Al atoms located along only the sinusoidal channels

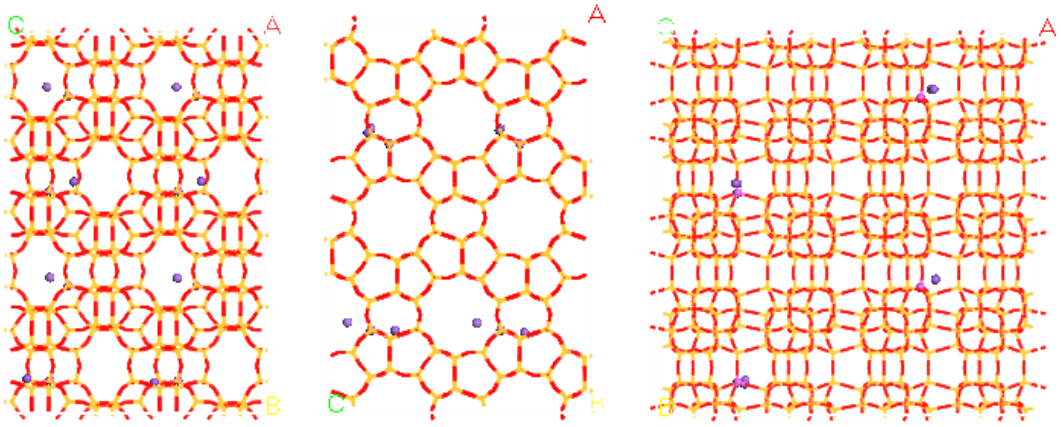

(a) **(b)** **(c)**

Figure 4.15 : A NaZSM-5 (95) composed of eight (2×2×2) unit cells along the (a) x-direction (b) y-direction (c) z-direction, Al atoms located along both elliptical and sinusoidal channels

A comparison between the resulting and the previous aqueous TCE adsorption isotherms in NaZSM-5 (95) is given in Figure 4.16-17. It is observed that the location of the Al atoms affect the characteristics of the adsorption isotherms. However, a clear conclusion cannot be made by considering only one comparison. Thus, further investigation is needed in future studies.

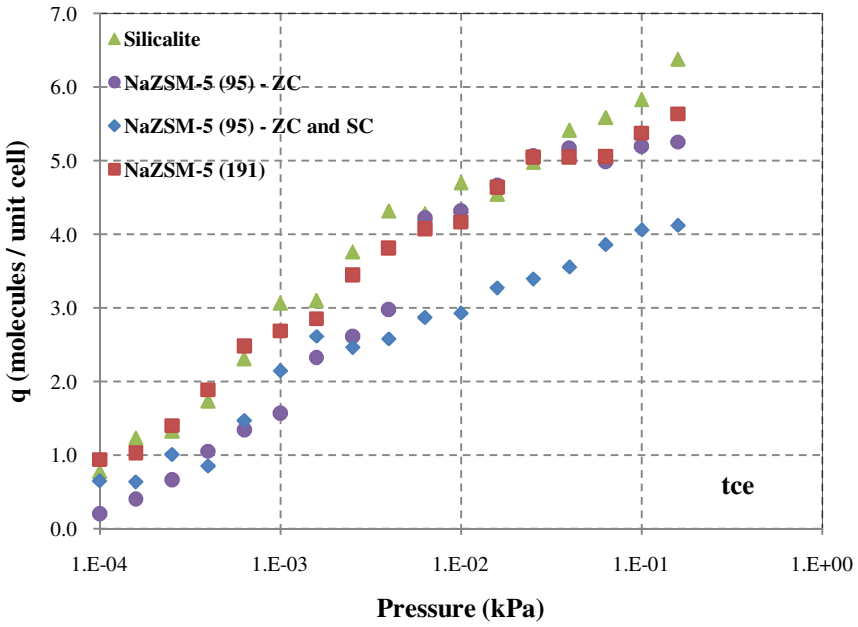

Figure 4.16 : Adsorption isotherms of aqueous TCE in NaZSM-5 (95) for different Al locations at 298K, compared to the previous isotherms

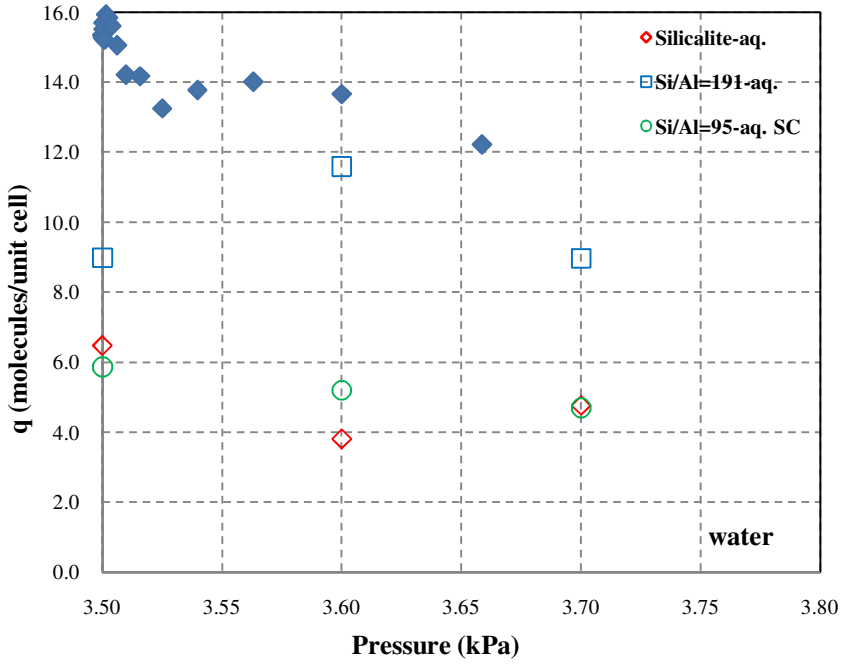

Figure 4.17 : Adsorption isotherms of water in NaZSM-5 (95) for different Al locations at 298K, compared to the previous isotherms

5. DIFFUSION SIMULATIONS

In this section, diffusion properties of pure and aqueous TCE in ZSM-5 zeolite and water diffusion in silicalite are investigated. Molecular dynamics (MD) method is used for the calculation of the diffusion coefficient, which is a dynamic property. Before MD, it is necessary to have a structure at equilibrium with guest molecules adsorbed. Here, guest molecules are TCE and water. Adsorption simulation is performed using Monte Carlo (MC) method. Afterwards, MD simulations are carried out and the diffusion properties of these molecules can be investigated.

5.1. Simulation Method

Sorption module in *Materials Studio 4.1* software is used to perform adsorption simulations. First, a single unit cell is extended along the z axis to form a 1x1x2 dimensioned super cell. 16 water molecules (8 water molecules per unit cell) are loaded to the super cell via Metropolis MC method. CVFF force field is used to represent the all bonded and non-bonded interatomic interactions, and the framework is kept flexible. The long-range interactions are calculated by Ewald summation method. Similarly, 4 TCE and 4 TCE plus 8 water molecules per unit cell are loaded into the ZSM-5 structures for pure and aqueous TCE mixtures, respectively. The temperature is fixed to 298K. As a result of these adsorption simulations, zeolite-guest molecule structures are formed (Figures 5.1-2).

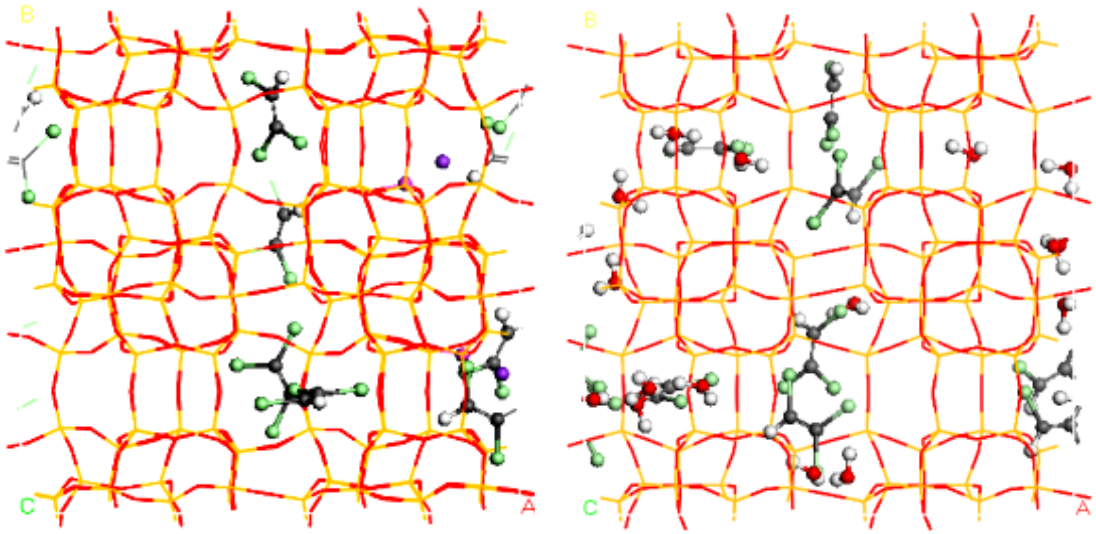

(a) **(b)**

Figure 5.1 : Two (1x1x2) unit cells of silicalite with (a) pure TCE (b) water and TCE molecules adsorbed

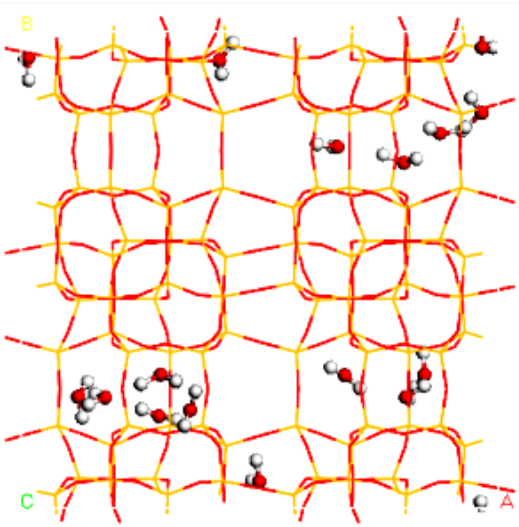

Figure 5.2 : Two (1x1x2) unit cells of silicalite with water molecules adsorbed

TCE diffusion simulations are performed in NaZSM-5 (95) and silicalite. On the other hand, water is diffused only into silicalite. TCE model used here is the same as the one in adsorption simulations. However, water model differs. Water molecules are represented by a single point charge (SPC) model, which is the default water model for CVFF [60]. Diffusion simulations are performed by using *Dynamics* option in *Discover* module.

The zeolite framework is assumed to be flexible in all simulations. All TCE diffusion simulations are performed in the NVT ensemble at 323K and 348K. The Velocity Verlet algorithm is used for numerical integration of motion with 250ps dynamics

time. Nosé thermostat [61] is selected. All the selections are the same for water diffusion simulations except that the temperature is fixed to 298K. Three consecutive MD runs are performed for TCE simulations, in order to obtain average data. On the other hand, two consecutive MD simulations are carried out for water. Each run lasts for 500.000 steps for equilibration, followed by 3 million steps for data acquisition.

It is aimed to observe diffusion characteristics of TCE depending on structure, water presence, and temperature. Moreover, the effect of changing charges of Si and O atoms on water diffusion in silicalite is investigated. q_{Si}/q_O=-2 ratio is preserved in order to conserve charge neutralization, and q_{Si} is set to six different values within the interval 0.6-1.2e where "e" indicates the elementary charge. Mean Square Displacement (MSD) - distance graphics are obtained using *Analysis* option. Average values are calculated for each simulation. The resulting graphics are linearly fitted. The overall diffusion coefficient values are obtained from the slopes of these graphics.

5.2. Results and Discussions

The resulting diffusion coefficients of TCE are compared in Figure 5.3. Numerical values can also be obtained from Table 5.1. It is observed that the presence of Al atoms, so Na^+ cations in the structure causes a decrease in diffusion velocity. This result is valid for both pure and aqueous diffusions. Furthermore, TCE diffusion slows down by the presence of water molecules, in both structures. Temperature only affects the diffusion of TCE from aqueous mixture into silicalite. At 348K, TCE molecules diffuse into silicalite faster than at 298K (Figure 5.3).

Table 5.1 : Numerical values for diffusion coefficients

D_0 (x10^{-10} m^2/s)				
Structure / Temperature	298K		348K	
	pure	**aqueous**	**pure**	**aqueous**
Silicalite – 1	2.147	1.302	2.185	2.165
NaZSM-5 (95)	1.427	1.025	1.435	1.128

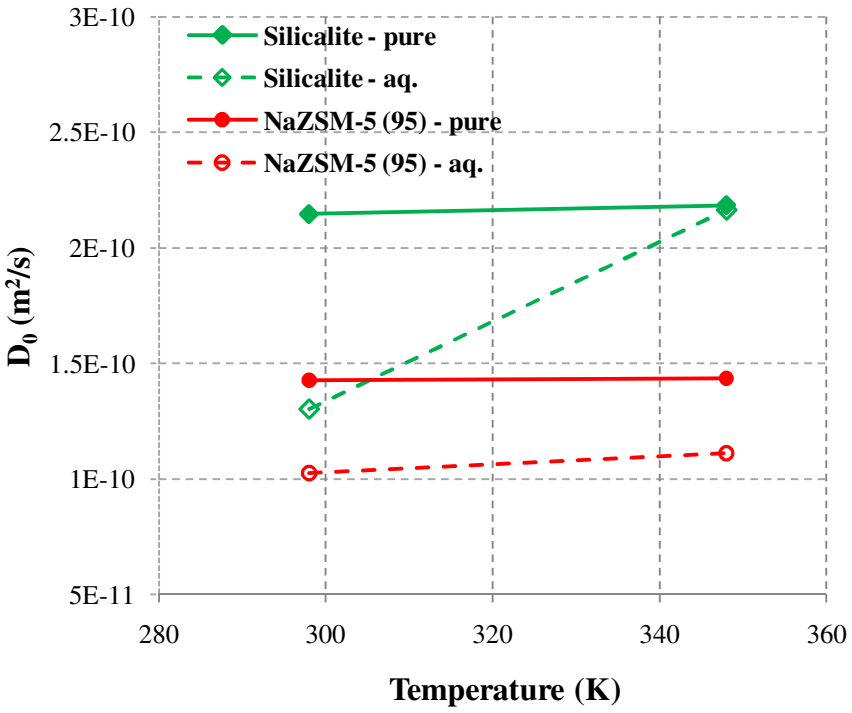

Figure 5.3 : Diffusion coefficients of TCE

In order to discover the diffusion properties of TCE in ZSM-5, concentration profiles are plotted with respect to adsorbate and zeolite type (Figures 5.4-5). Water causes a drift in the locations of the TCE molecules. This is not observed in the adsorption simulations where the zeolite structure is rigid. However, TCE molecules are still mostly present in the straight channels as they were in the adsorption stage.

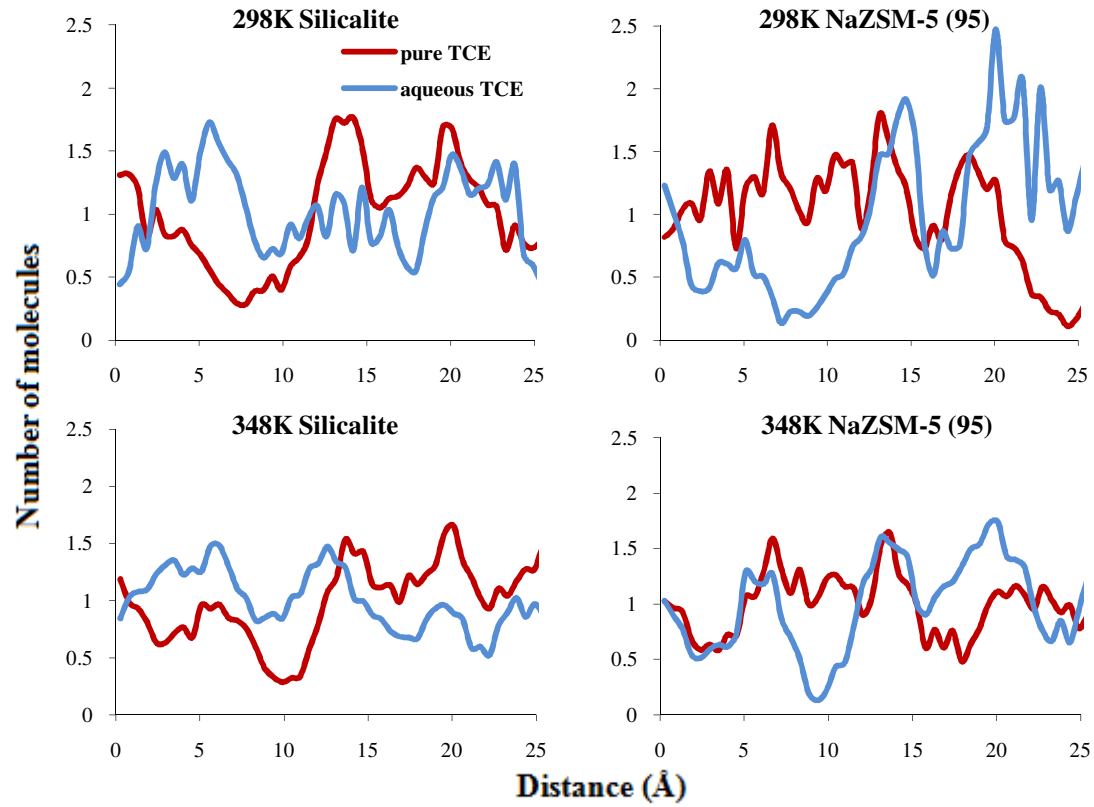

Figure 5.4 : Concentration profiles of TCE diffused into ZSM-5 zeolites at 298K and 348K, with respect to adsorbed TCE

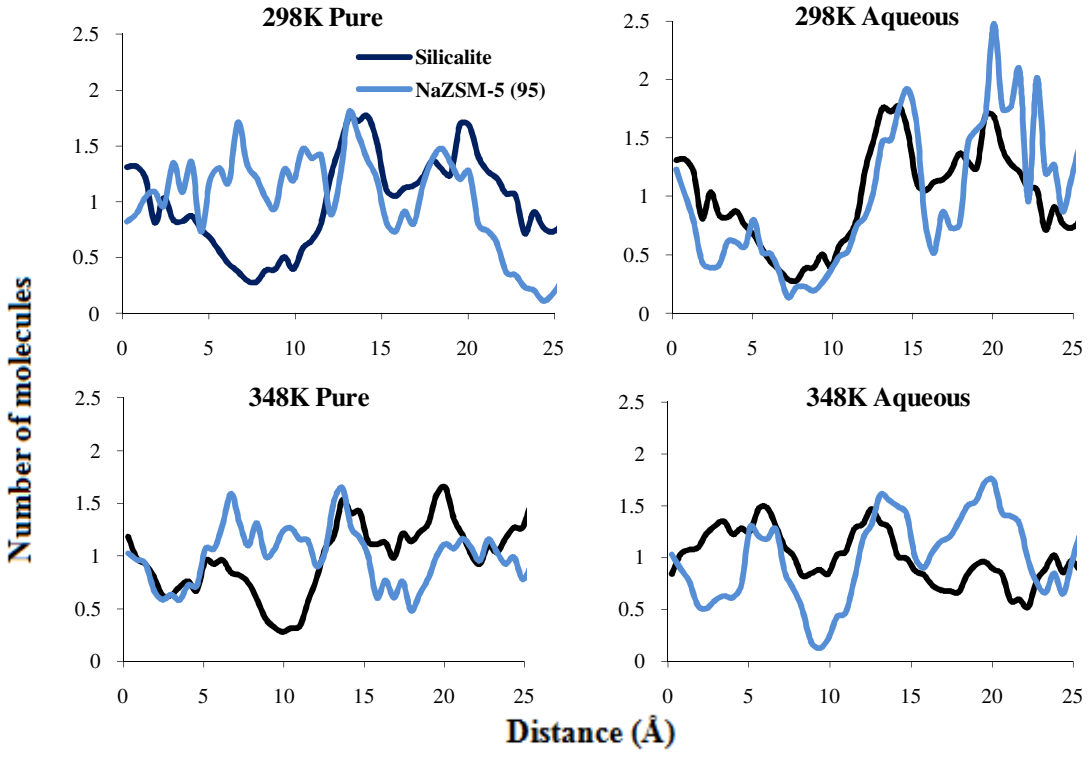

Figure 5.5 : Concentration profiles of TCE diffused int ZSM-5 zeolites at 298K and 348K, with respect to zeolite type

Average MSD-distance relations for water diffusions in silicalite depending on Si charges are displayed in Figure 5.6. Diffusion coefficients are calculated for two additional Si charges in order to obtain intermediate diffusion coefficient values for better interpretation (Figure 5.7). The results are compared with previous theoretical [46,53,62,63] and experimental [64] studies in Table 5.2.

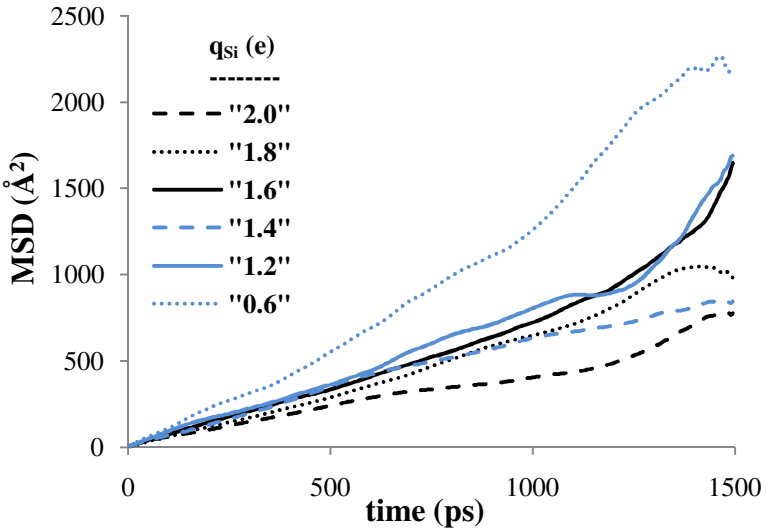

Figure 5.6 : MSD-time graphics of TCE for different electrostatic charges of silicon atoms

Analysis on Figure 5.7 show that the diffusion coefficient of water decreases significantly with increasing partial charge of Si atoms, when the charges of the Si atoms are below 1.4e. Above 1.4e, the diffusion coefficient remains relatively constant. Furthermore, the diffusivity values for $q_{Si} \geq 1.4e$ are in agreement with the experimental data (Table 5.2). This observation may be related to the previous MD study of Desbiens *et al.* [24], where it was concluded that the partial charge of Si atoms should be kept below approximately 1.7e in order to prevent a condensation phenomenon at a gas pressure below the saturation pressure of the bulk water.

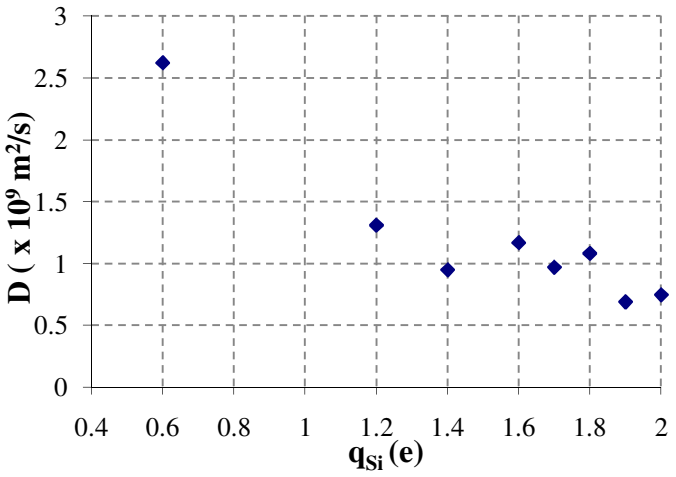

Figure 5.7 : Diffusion coefficient distribution of TCE depending on the partial charge of Si atoms in silicalite framework

Table 5.2 : Diffusion coefficient values of water compared to former studies

	this work		Ref.62	Ref.46	Ref.63	Ref.53	Ref.64 (exp. by PFG-NMR)
T (K)	298		297	297	300	298	297
q_{Si} (elementary charges)	0.60	1.20	0.89	0.89	2.00	1.67/1.57	-
D (x 10^9 m^2/s)	2.62	1.31	1.94	8.83	8.61	3.30	1.70

Concentration profiles of water molecules give detailed information about water behavior in ZSM-5 zeolites (Figure 5.8). It is worth to note that the concentration profile at q=1.6e matches up with the work of Arı et al. [62] (Figure 5.9), where they carried out MD simulations at 297K using COMPASS forcefield with the default partial charge of silicon atoms set as 0.89e. This current study is in agreement with their work that water molecules are mostly adsorbed in the straight channels.

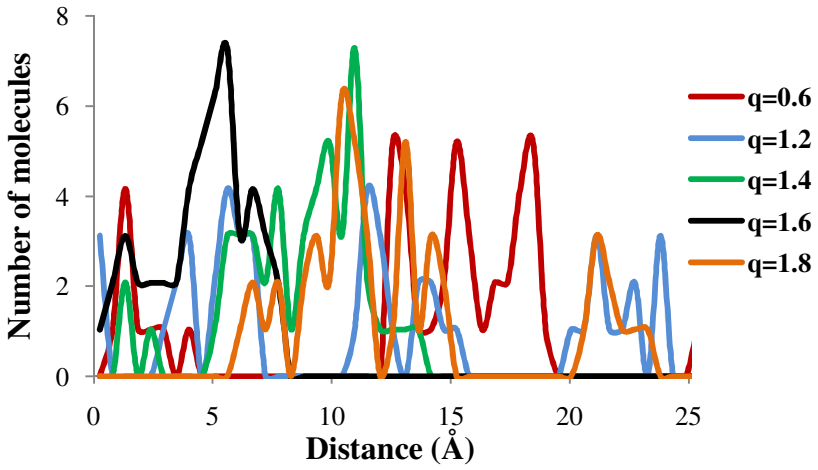

Figure 5.8 : Concentration profiles of water molecules diffused into silicalite

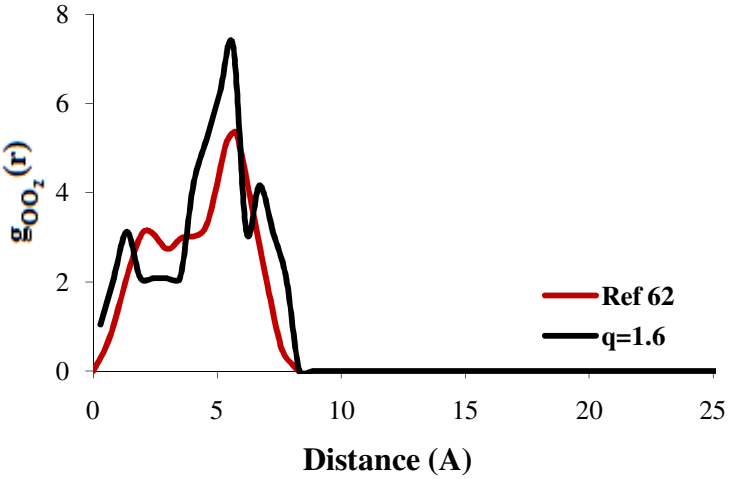

Figure 5.9 : Comparison of RDFs of oxygen atoms in water molecules diffused into silicalite

RDFs of oxygen atoms in water molecules are plotted in Figure 5.10. Within the interval 4-6Å, closer analysis of the RDFs shows that water molecules exhibit an ordered structure for partial charges of silicon atoms smaller than 1.8e. For larger charges, there is not an ordered structure formed by the water molecules.

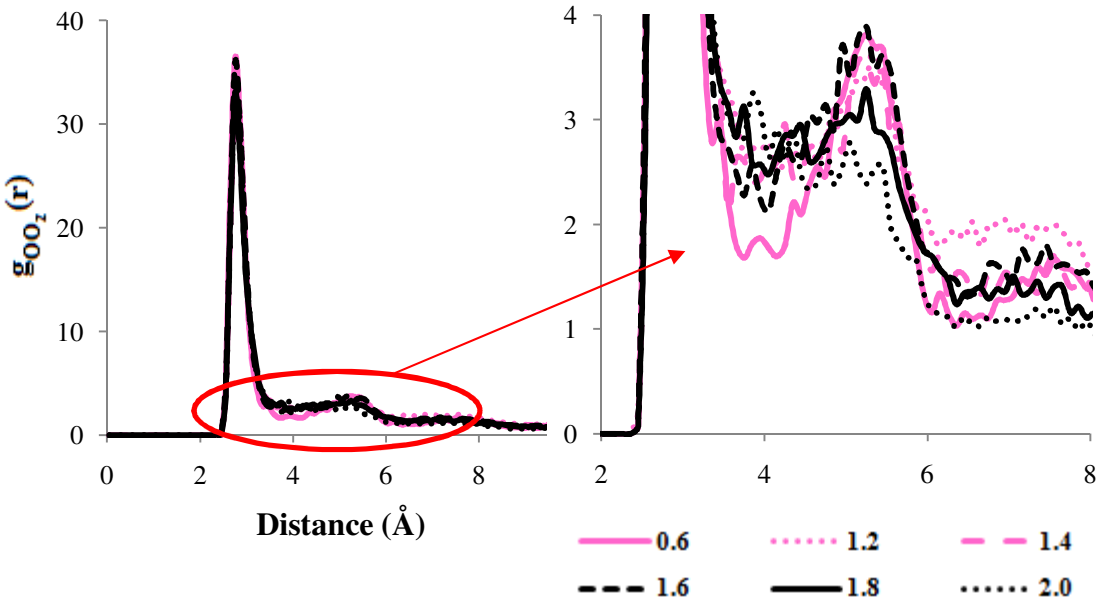

Figure 5.10 : RDFs of oxygen atoms in water molecules diffused into silicalite framework with different partial charges of Silicon atoms

6. CONCLUSIONS

Methyl tertiary butyl ether (MTBE) and trichloroethylene (TCE) are volatile organic compounds (VOCs) which have been used in industry. Since they had been found harmful to human health when mixed in drinking water sources, their removal from water has become an important issue. The widely used methods for the removal of these VOCs are adsorption by activated carbon and hydrophobic materials like zeolites. Up to date, experimental studies on these issues are present, but there are a few theoretical studies. This work investigates the MTBE adsorption in faujasites and TCE adsorption and diffusion in ZSM-5 and faujasites by the use of molecular simulations.

Monte Carlo (MC) and molecular dynamics (MD) method are used to study adsorption and diffusion of MTBE and TCE in zeolites. The mainly investigated points are the effects of water, Si/Al ratio and temperature on the adsorption characteristics of MTBE and TCE.

The adsorption capacity of MTBE in faujasites is not affected from the extraframework cations, except for low pressures. High Si/Al ratio is found to decrease the adsorption capacity at low pressures, but it does not change the saturation capacity. Organophilicity increases with decreasing aluminum content. Similarly, temperature decreases MTBE adsorption capacity below the saturation pressure, while the saturation capacity remains unchanged, as expected. This is an advantage for MTBE removal, because low temperature means less energy and money consumption.

TCE adsorption simulations performed in this study are in agreement with both experimental and theoretical results. Simulations show that as aluminum content increases, TCE adsorption capacity decreases significantly at moderate vapor pressures of TCE. Therefore, the performance of the zeolite for the removal of TCE from water will be the highest when the framework contains no aluminum. Moreover, the presence of water decreases TCE adsorption significantly, water

molecules replace TCE molecules in zeolite pores as pressure increases. However, the water adsorption capacity of ZSM-5 does not monotonically increase with decreasing Si/Al ratio. This may be attributed to the location of Al atoms in the framework. Simulations in this study show that their location can significantly alter the water adsorption capacity: Simulation with zeolite structure with the same Si/Al ratio (95) and aluminum atoms being located on different channels, results in different adsorption characteristics. Therefore, a more rigorous study on the effect of the Al-atom locations on the adsorption capacity is required in the future.

TCE molecules are observed mostly in the straight channels and the intersections, for all ZSM-5 structures due to their size. Water effect is not found to be significant. Only in silicalite, water molecules form clusters where they populate. In NaZSM-5 zeolites, water molecules mostly populate near the cations.

TCE adsorption simulations in faujasites showed that while the CVFF forcefield correctly estimates the saturation capacity of the zeolite, it underestimates the adsorbed amount at lower pressures. Thus, a more accurate forcefield is required to represent TCE-faujasite interactions. However, a sudden increase in the adsorption capacity of the faujasite is observed when the framework is changed from DAY to NaY48, which shows the significant effect of the Al atoms. Moreover, TCE molecules are found to be homogenously adsorbed into the pores in all structures.

The diffusion characteristics of pure TCE and its aqueous mixture are also considered in this study. It is seen that the presence of aluminum atoms reduces the diffusion rate of both pure and aqueous TCE. Besides, water molecules cause a decrease in TCE diffusion rate. Water molecules are found to cause a drift in the locations of the TCE molecules in diffusion simulations. However, TCE molecules are still mostly present in the straight channels. The studied temperatures do not affect diffusion significantly, except for the diffusion coefficient of aqueous TCE in silicalite that increases with temperature.

Adsorption and diffusion properties of water in silicalite have become an important issue as silicalite is used in the applications of organics removal from water. The hydrophobicity of silicalite makes it more significant. Water diffusion in silicalite is simulated separately in this study, as a function of partial charge of silicon atoms in the framework. It is concluded that diffusion coefficient of water decreases by the increasing charge values, up to 1.4e. This result is in agreement with the previous

experimental and theoretical studies. For higher partial charge values, diffusion coefficient remains relatively constant. It is also noted that water molecules exhibit an ordered structure for partial charges of silicon atoms smaller than 1.8e, which may be related to the condensation of water molecules in the zeolite pores. For more accurate results, studies with Al substituted ZSM-5 frameworks should be performed.

REFERENCES

[1] **U.S. EPA OEHHA,** 1999. Public Health Goal for Trichloroethylene in Drinking Water, California.

[2] **U.S. EPA,** 2007. Toxicity and Exposure Assessment for Children's Health, United States.

[3] **Shim, W. G., Lee, J. W., Rhuee, H., Moon, H.,** 2004: Adsorption Dynamics for the Capillary Condensation of Trichloroethylene Vapor on Mesoporous Material. *Korean J. Chem. Eng*., Vol **21**(2), no. 2, pp. 469-476.

[4] **U.S. EPA website** <http://www.epa.gov/ttn/atw/hlthef/tri-ethy.html>, accessed at 27.10.2009.

[5] **U.S. EPA website** <http://www.epa.gov/safewater/contaminants/dw_contamfs/trichlor.html>, accessed at 27.10.2009.

[6] **Pascual, P., Ungerer, P., Tavitian, B., and Boutin, A.,** 2004: Development of a Tansferable Guest-Host Force Field for Adsorption of Hydrocarbons in Zeolites. II. Prediction of Alkenes Adsorption and Alkane/Alkene Selectivity in Silicalite. *J. Phys. Chem. B.* Vol **108,** no. 1, pp. 393-398.

[7] **Pascual, P., Ungerer, P., Tavitian, B., Pernot, P., and Boutin, A.,** 2003: Development of a transferable guest-host force field for adsorption of hydrocarbons in zeolites. I. Reinvestigation of alkane adsorption in silicalite by grand canonical Monte Carlo simulation. *Phys. Chem. Chem. Phys.,* **5,** 3684-3693.

[8] **Tanada, S., Nakamura, T., Xiaohong, M., Higuchi, T., Shinoda, S.,** 1992: Adsorption Characteristics of Trichloroethylene and 1,1,1-Trichloroethane onto Activated Carbon Fiber in Gaseous Phase. *Bull. Environ. Contain. Toxicol.,* Vol **49**, pp. 112-119.

[9] **University of Minnesota website** <http://horticulture.cfans.umn.edu/vd/h5015/99fpapers/tlusty.htm>, accessed at 2.11.2009.

[10] **Mellot, C. F., Cheetham, A. K., Harms, S., Gorte, R. J., Myers, A. L.,** 1998: Calorimetric and Computational Studies of Chlorocarbon Adsorption in Zeolites. *J. Am. Chem. Soc.* Vol **120,** 5788-5792.

[11] **Ahunbay, M. G.,** 2007: Molecular simulation of adsorption and diffusion of chlorinated alkenes in ZSM-5 zeolites. *J. Chem. Phys.* Vol. **127,** no. 4, pp. 44707/1-6.

[12] **U.S. EPA website** <www.epa.gov/mtbe>, accessed at 27.10.2009.

[13] **U.S. EPA HECD Office of Water,** 1997: Drinking Water Advisory: Consumer Acceptability Advice and Health Effects Analysis on Methyl Tertiary-

Butyl Ether (MtBE), *EPA Advisory* Report, **EPA-822-F-97-009,** Washington, D.C.

[14] **Asian Clean Fuels Association website** <http://www.acfa.org.sg/pdf/MTBE%20Supply%20Demand%20&%20Industry%20Outlook.pdf>, accessed at 27.10.2009.

[15] **U.S. EPA OEHHA,** 1999. Public Health Goal for Methyl Tertiary Butyl Ether (MTBE) in Drinking Water, California.

[16] **Erdal, S., and Goldstein, B. D.,** 2000: Methyl tert-Butyl Ether as a Gasoline Oxygenate: Lessons for Environmental Public Policy, *Annu. Rev. Energy Environ.,* **25,** 765-802.

[17] **Anderson, M. A.,** 2000: Removal of MTBE and Other Organic Contaminants from Water by Sorption to High Silica Zeolites. *Environ. Sci. Technol.* Vol. **34,** no. 4, pp. 725-727.

[18] **Yazaydin, A. Ö.,** 2007. Molecular Simulation of the Adsorption of Organics From Water, *PhD Thesis,* Worcester Polytechnic Institute, Worcester.

[19] **Narusawa, K.,** (2007). Past experience in improved fuel quality in Japan. *File of Oral Presentation.* Retrieved September 25, 2008, from http://www.unece.org/trans/doc/2007/wp29/Presentation%20Japan.pdf.

[20] **Sutherland, J., Adams, C., and Kekobad, J.,** 2004: Treatment of MTBE by air stripping, carbon adsorption, and advanced oxidation: technical and economic comparison for five groundwaters, *Water Research,* **38,** 193-205.

[21] **Acero, J. L., Haderlein, S. B., Schmidt, T. C., Suter, M. J. F., and von Gunten, U.,** 2001: MTBE Oxidation by Conventional Ozonation and the Combination Ozone/Hydrogen Peroxide: Efficiency of the Processes and Bromate Formation. *Environ. Sci. Technol.* Vol. **35,** no. 21, pp. 4252-4259.

[22] **Ungerer, P., Nieto-Draghi, C., Rousseau, B., Ahunbay, G., and Lachet, V.,** 2007: Molecular simulation of the thermophysical properties of fluids: From understanding toward quantitative. *Journal of Molecular Liquids,* **134,** 71-89.

[23] **Smit, B., Krishna, R.,** 2001: Monte Carlo simulations in zeolites. *Current Opinion in Solid State and Materials Science,* **5,** 455-461.

[24] **Fuchs, A. H., Cheetham, A. K.,** 2001: Adsorption of Guest Molecules in Zeolitic Materials: Computational Aspects. *J. Phys. Chem. B,* **105,** 31.

[25] **Auerbach, S. M., Carrado, K. A., and Dutta, P. K.,** 2003: Handbook Of Zeolite Science and Technology. Marcel Dekker, New York.

[26] **Garrot, B., Simonot-Grange, M-H., Clausse, B.,** 1999: Use of dealuminated faujasite Y and ZSM-5 zeolites for VOC's adsorption. Application of air cleaning. *Porous Materials in Environmentally Friendly Processes,* **125,** 683-690.

[27] **Bouvier, F., Weber, G.,** 1998: Adsorption of a polar or non-polar chloroalkene on a ZSM-5 zeolite at 298K. *Journal of Thermal Analysis,* **54,** 881-889.

[28] **Clausse, B., Garrot, B., Cornier, C., Paulin, C., Simonot-Grange, M-H., Boutros, F.,** 1998: Adsorption of chlorinated volatile organic compounds on hydrophobic faujasite: correlation between the thermodynamic and kinetic properties and the prediction of air cleaning. *Microporous and Mesoporous Materials,* **25,** 169-177.

[29] **Giaya, A., Thompson, R. W. Denkewicz Jr., R.,** 2000: Liquid and vapor phase adsorption of chlorinated volatile organic compounds on hydrophobic molecular sieves. *Microporous and Mesoporous Materials,* **40,** 205-218.

[30] **Giaya, A., Thompson, R. W.,** 2002: Single-component gas phase adsorption and desorption studies using a tapered element oscillating microbalance. *Microporous and Mesoporous Materials,* **55,** 265-274.

[31] **Chihara, K., Terakado, T., Ninomiya, T., Mizuochi, H.,** 2004: Chromatographic adsorption measurement of chlorinated organics on high silica zeolite. *Studies in Surface Science and Catalysis,* **154,** 1991-1998.

[32] **Noack, M., Kölsch, P., Caro, J., Schneider, M., Toussaint, P., Sieber, I.,** 2000. MFI membranes of different Si/Al ratios for pervaporation and steam perpeation. *Microporous and Mesoporous Materials,* **35-36,** 253-265.

[33] **Li, S., Tuan., V. A., Noble, R. D., Falconer, J. L.,** 2003: MTBE Adsorption on All-Silica beta Zeolite. *Environ. Sci. Technol.,* **37,** 4007-4010.

[34] **Erdem-Şenatalar, A., Bergendahl, J. A., Giaya, A., and Thompson, R. W.,** 2004: Adsorption of Methyl Tertiary Butyl Ether on Hydrophobic Molecular Sieves. *Environmental Engineering Science.* Vol. **21,** no. 6, pp. 722-729.

[35] **Knappe, D. R. U., Campos, A. A. R.,** 2005: Effectiveness of high-silica zeolites for the adsorption of methyl tertiary-butyl ether from natural water.. *Water Sci. And Tech.: Water Supply,* 5, 83.

[36] **Rossner, A., and Knappe, D. R. U.,** 2008: MTBE adsorption on alternative adsorbents and packed bed adsorber performance, *Water Research,* **42,** 2287-2299.

[37] **Gironi, F., Capparucci, C., and Marrelli, L.,** 2003: Adsorption of MTBE Vapors onto Activated Carbon. *J. Chem. Eng. Data.* Vol. **48,** no. 4, pp. 783-788.

[38] **Yazaydın, A. Ö., and Thompson, R. W.,** 2006: Molecular Simulation of the Adsorption of MTBE in Silicalite, Mordenite, and Zeolite Beta. *J. Phys. Chem. B.* Vol. **110,** no. 29, pp. 14458-14462.

[39] **Hill, J. R., and Sauer, J.,** 1994: Molecular Mechanics Potential for Silica and Zeolite Catalysts Based on ab Initio Calculations. 1. Dense and Microporous Silica. *J. Phys. Chem.* Vol. **98,** no. 4, pp. 1238-1244.

[40] **Ahunbay, M. G., Karvan, O., and Erdem-Şenatalar, A.,** 2008: MTBE adsorption and diffusion in silicalite, *Microporous and Mesoporous Materials,* **115,** 93-97.

[41] **Sadus, R. J.,** 2002: Molecular Simulation of Fluids Theory, Algorithms and Object-Orientation. Elsevier, Amsterdam.

[42] **Cundari, T. R.,** 2001: Computational Organometallic Chemistry. Marcel Dekker, New York.

[43] **Di Lella, A., Desbiens, N., Boutin, A., Demachy, I., Ungerer, P., Bellat, J-P., Fuchs, A. H.,** 2006: Molecular simulation studies of water physisorption in zeolites. *Phys. Chem. Chem Phys.,* **8,** 5396-5406.

[44] **Auerbach, S. M., Henson, N. J., Cheetham, A. K., Metiu, H. I**., 1995: Transport Theory for Cationic Zeolites: Diffusion of Benzene in Na-Y. *J. Phys. Chem.,* **99,** 10600-10608.

[45] **Jaramillo, Grey, C. P., Auerbach, S. M.,** 2001: Molecular Dynamics Studies of Hydrofluorocarbons in Faujasite-type Zeolites: Modeling Guest-Induced Cation Migration in Dry Zeolites. *J. Phys. Chem. B,* **105,** 12319-12329.

[46] **Krokidas, P., Skouras, E. D., Nikolakis, V., Burganos, V. N.,** 2008: Simulated annealing effects on Na-FAU crystal reconstruction and sorption efficiency. *Molecular Simulation,* **34,** 10-15, 1299-1309.

[47] **Frenkel, D., and Smit, B.,** 2002: Understanding Molecular Simulation From Algorithms to Applications. Academic Press, San Diego.

[48] **Ungerer, P., Tavitian, B., and Boutin, A.,** 2005: Applications of Molecular Simulation in the Oil and Gas Industry - Monte Carlo Methods. Editions Technip, Paris.

[49] **Fleys, M., Thompson, R. W., MacDonald, J. C.,** 2004: Comparison of the Behavior of Water in Silicalite and Dealuminated Zeolite Y at Different Temperatures by Molecular Dynamic Simulations. *J. Phys. Chem B,* **108,** 12197-12203.

[50] **Lumey, M-W., Melin, T.,** 2008: Molecular simulations on the selectivity of a zeolite membrane. *Desalination,* **224,** 119-123.

[51] **Desbiens, N., Boutin, A., Demachy, I.,** 2005: Water Condensation in Hydrophobic Silicalite Zeolite: A Molecular Simulation Study. *J. Phys. Chem. B,* **109,** 24071-24076.

[52] **Accelrys Materials Studio 4.1**, www.accelrys.com, accessed at 12.11.2009.

[53] **Bussai, C., Fritzsche, S., Haberlandt, R., Supot, H.,** 2003: Formation of Low-Density Water Clusters in the Silicalite Cage: A Molecular Dynamics Study. *J. Phys. Chem. B,* **107,** 12444-12450.

[54] **Baerlocher, C., Meier, W. M., and Olson, D. H.,** 2001: Atlas of Zeolite Framework Types. Elsevier, Amsterdam.

[55] **Buttefey, S., Boutin, A., Mellot-Draznieks, C., Fuchs, A. H.,** 2001: A Simple Model for Predicting the Na^+ Distribution in Anhydrous NaY and NaX Zeolites. *J. Phys. Chem. B,* **113,** 8073-8079.

[56] **Güvenç, E.,** 2009. Molecular Modeling of Ether Adsorption In ZSM-5 Zeolites, *MA Thesis,* Istanbul Technical University, Istanbul.

[57] **Errington J.R., Panagiotopoulos A.Z.,** 1998: A Fixed Point Charge Model for Water Optimized to the Vapor-Liquid Coexistence Properties, *J. Phys. Chem. B*., **102,** 7470-7475.

[58] **Wender, A., Barreau, A., Lefebvre, C., Di Lella, A., Boutin, A., Ungerer, P., Fuchs, A. H.,** 2007: Adsorption of n-alkanes in faujasite zeolites: Molecular simulation study and experimental measurements. *Adsorption,* **13,** 439-451.

[59] **Martin M. G.,** 2006. Comparison of the AMBER, CHARMM, COMPASS, GROMOS, OPLS, TraPPE ve UFF force fields for prediction of vapor–liquid coexistence curves ve liquid densities, *Fluid phase equilibria,* **248**, 50-55.

[60] **Dauber-Osguthorpe, P., Roberts, V. A., Osguthorpe, D. J., Wolff, J., Genest, M., and Hagler, A. T.,** 1988: Structure and energetics of ligand binding to proteins: *Escherichia coli* dihydrofolate reductase-trimethoprim, a drug-receptor system. *Proteins: Struct. Funct. Genet.* Vol. **4,** no. 1, pp. 31-47.

[61] **Nose S.,** 1984. A unified formulation of the constant temperature dynamics methods, *Journal of Chemical Physics,* **81,** 511-519.

[62] **Arı, M., Ahunbay, M. G., Yurtsever, M., Erdem-Şenatalar, A.,** 2009: Molecular Dynamics Simulation of Water Diffusion in MFI-Type Zeolites. *J. Phys. Chem.*, in preparation.

[63] **Demontis, P., Stara, G., Suffritti, G. B.,** 2003: Behavior of Water in Hydrophobic Zeolite Silicalite at Different Temperatures. A Molecular Dynamics Study. *J. Phys. Chem. B,***107,** 4426-4436.

[64] **Bussai, C., Vasenkov, S., Liu, H., Böhlmann, W., Fritzsche, S., Hannongbua, S., Haberlandt, R., Karger, J.,** 2002: On the diffusion of water in silicalite: MD simulations using ab initio fitted potential and PFG NMR measurements. *App. Catal. A: Gen.,* **232,** no. 1-2, pp. 59-66.

CURRICULUM VITAE

Candidate's full name: Melissa KARAGÖZLÜOĞLU

Place and date of birth: Beyoğlu/İstanbul-26.12.1984

Permanent Address: Duatepe Mah. Savaş Sok. No:11/3 Bahar Apt. Şişli-İstanbul

Universities and Colleges attended:

B.Sc. : Physics Engineering, İstanbul Technical University (2002-2006)

Chemical Engineering, İstanbul Technical University (2004-2008)

M.Sc. : Chemical Engineering, İstanbul Technical University (2008-2010)